

MOL # 87783

TITLE PAGE

The pharmacology of a potent and selective agonist, TUG-891, demonstrates both potential opportunity and possible challenges to therapeutic agonism of FFA4 (GPR120)

**Brian D. Hudson, Bharat Shimpukade, Amanda E. Mackenzie, Adrian J. Butcher, John D. Pediani,
Elisabeth Christiansen, Helen Heathcote, Andrew B. Tobin, Trond Ulven, and Graeme Milligan**

Molecular Pharmacology Group, Institute of Molecular, Cell and Systems Biology, College of Medical,
Veterinary and Life Sciences, University of Glasgow, Glasgow G12 8QQ, Scotland, United Kingdom
(BDH, AEM, JDP, HH, GM);

Department of Physics, Chemistry and Pharmacy, University of Southern Denmark, Campusvej 55, DK-
5230 Odense M (BS, EC, TU);

MRC Toxicology Unit, University of Leicester, Leicester, LE1 9HN, United Kingdom (AJB, ABT)

MOL # 87783

Running title: The therapeutic potential of FFA4

To whom correspondence should be addressed: Graeme Milligan, Wolfson Link Building 253, University of Glasgow, Glasgow G12 8QQ, Scotland, U.K. Tel +44 141 330 5557, FAX +44 141 330 5481, e-mail:

Graeme.Milligan@glasgow.ac.uk

Manuscript information

Text Pages:	44
Tables:	1
Figures:	10
Words in Abstract:	248
Words in Introduction:	804
Words in discussion:	1745
References	42

Nonstandard Abbreviations: aLA, α -linolenic acid; DHA, docosahexaenoic acid; eYFP, enhanced yellow fluorescent protein; FFA, free fatty acid; GLP-1, glucagon-like peptide-1; GPCR, G protein-coupled receptor; GSIS, glucose stimulated insulin secretion; LCFA, long chain fatty acid; TNF, tumor necrosis factor;

Chemical names: GW9508, (4-[[[3-phenoxyphenyl)methyl]amino]benzenepropanoic acid); GW1100 (4-[5-[(2-ethoxy-5-pyrimidinyl)methyl]-2-[[[4-fluorophenyl)methyl]thio]-4-oxo-1(4H)-pyrimidinyl]-benzoic acid, ethyl ester); NCG21 ((4-{4-[2-(phenyl-2-pyridinylamino)ethoxy]phenyl)butyric acid)), TUG-891, (3-(4-((4-fluoro-4'-methyl-[1,1'-biphenyl]-2-yl)methoxy)phenyl)-propanoic acid); TUG-905 (3-(2-fluoro-4-(((2'-methyl-4'-(3-(methylsulfonyl)propoxy)-[1,1'-biphenyl]-3-yl)methyl)amino)-phenyl)propanoic acid); Iressa (N-(3-chloro-4-fluoro-phenyl)-7-methoxy-6-(3-morpholin-4-ylpropoxy)quinazolin-4-amine)

MOL # 87783

Abstract

TUG-891 was recently described as a potent and selective agonist for the long chain fatty acid (LCFA) receptor FFA4 (previously GPR120). Herein we have used TUG-891 to further define the function of FFA4 and used this compound in proof of principle studies to indicate the therapeutic potential of this receptor. TUG-891 displayed similar signaling properties to the LCFA α -linolenic acid at human FFA4 across various assay endpoints, including stimulation of Ca^{2+} mobilization, β -arrestin-1 and β -arrestin-2 recruitment and extracellular signal-regulated kinase phosphorylation. Activation of human FFA4 by TUG-891 also resulted in rapid phosphorylation and internalization of the receptor. While these latter events were associated with desensitization of the FFA4 signaling response, removal of TUG-891 allowed both rapid recycling of FFA4 back to the cell surface and resensitization of the FFA4 Ca^{2+} signaling response. TUG-891 was also a potent agonist of mouse FFA4, however it showed only limited selectivity over mouse FFA1, complicating its use *in vivo* in this species. Pharmacological dissection of responses to TUG-891 in model murine cell systems indicated that activation of FFA4 was able, however, to mimic many potentially beneficial therapeutic properties previously reported for LCFAs, including stimulating glucagon-like peptide-1 secretion from enteroendocrine cells, enhancing glucose uptake in 3T3-L1 adipocytes, and inhibiting release of pro-inflammatory mediators from RAW 264.7 macrophages; suggesting promise for FFA4 as a therapeutic target for type 2 diabetes and obesity. Together, these results demonstrate both potential but also significant challenges that still need to be overcome in order to therapeutically target FFA4.

MOL # 87783

Introduction

Fatty acids are important biological molecules that serve both as a source of energy and as signaling molecules regulating metabolic and inflammatory processes. In the past fatty acids were believed to produce their biological effects through interacting with intracellular targets including, for example, the family of peroxisome proliferator-activated receptors. However, in recent years it has become clear that fatty acids also serve as agonists for a group of cell surface G protein-coupled receptors (GPCRs). These include three closely related receptors designated as a free fatty acid (FFA) receptor family: FFA1 (previously GPR40), FFA2 (previously GPR43) and FFA3 (previously GPR41) (Stoddart et al., 2008a); as well as two additional, structurally more distantly related, GPCRs GPR120 (Hirasawa et al., 2005) and GPR84 (Wang et al., 2006). While the relevance of fatty acid ligands on GPR84 remains uncertain, the ability of LCFAs to activate GPR120 is now well established (Hirasawa et al., 2005; Oh et al., 2010). As a result, despite limited homology with the other family members, GPR120 has recently been added to the FFA family of receptors and is now designated FFA4.

Since the deorphanization of the FFA receptor family members, these receptors have been implicated in many of the biological effects of fatty acids on both metabolic and inflammatory processes and, as a consequence, great interest has accrued in developing novel pharmacological reagents to assess the therapeutic potential of these receptors (Holliday et al., 2011; Ulven, 2012; Hudson et al., 2013b). To date, FFA1 has received the greatest attention based on clear validation as a target for the treatment of type 2 diabetes, due to its ability to enhance glucose stimulated insulin secretion (GSIS) (Itoh et al., 2003) and at least one FFA1 agonist has progressed through phase II clinical trials for this prospective end-point (Burant et al., 2012; Kaku et al., 2013). However, interest in FFA4 has also been steadily growing, again for the treatment of type 2 diabetes and/or obesity. Early studies indicated that FFA4 is expressed highly in enteroendocrine cells and suggested that it may mediate LCFA-stimulated release of glucagon-like peptide-1 (GLP-1) from these cells (Hirasawa et al., 2005). Furthermore, FFA4 expressed by adipocytes is reported to enhance glucose uptake, while in macrophages activation of FFA4 appears to be anti-inflammatory, and hence promotes improved insulin sensitivity (Oh et al., 2010). Moreover, recent data

MOL # 87783

suggests FFA4 is expressed in the pancreas and that it can protect pancreatic islets from palmitate-induced apoptosis (Taneera et al., 2012). Taken together, these findings suggest FFA4 may play important roles in both metabolic and inflammatory processes associated with the development of type 2 diabetes and that agonism of this receptor could represent a promising and novel therapeutic approach.

Further support for FFA4 as a therapeutic target has come recently from genetic studies in both mice and humans, showing that mice genetically lacking the receptor or humans possessing an FFA4 polymorphism with reduced signaling activity are both prone to obesity (Ichimura et al., 2012). However, despite all of these promising and tantalizing findings, a lack of synthetic ligands with high potency and selectivity for FFA4 has meant that many of the previous studies have been indirect or have relied on the use of fatty acids only as ligands. This has greatly limited proof of principle studies to validate FFA4 more fully as a therapeutic target. In particular, identifying ligands with suitable selectivity for FFA4 over the other LCFA receptor, FFA1, has been challenging (Hudson et al., 2011). Early FFA4 ‘selective’ compounds reported in the academic literature displayed only poor potency and very limited selectivity over FFA1 (Suzuki et al., 2008; Hara et al., 2009a). However, we have recently reported a highly potent and selective agonist of FFA4, with TUG-891 (Shimpukade et al., 2012) potentially offering a suitable tool compound with which to selectively probe FFA4 function.

In the present study we examine, therefore, the *in vitro* function of TUG-891 in cells transfected to express species orthologs of the receptor. We demonstrate that this ligand possesses similar signaling properties to the endogenous fatty acids at FFA4 but with significantly greater potency and selectivity. We establish that this ligand can be used to examine FFA4 function in cells endogenously expressing the receptor, and that it produces many of the beneficial properties previously associated with activation of the receptor, including stimulating GLP-1 release, enhancing glucose uptake and inhibiting pro-inflammatory cytokine secretion. However, as noted in early studies (Hirasawa et al., 2005; Fukunaga et al. 2006; Watson et al. 2012), agonist treatment results in rapid and extensive removal of FFA4 from the surface of cells and we now also demonstrate desensitization of functional responses. Although this may pose challenges for the therapeutic development of FFA4 agonists, we also observe that functional

MOL # 87783

responses are rapidly re-established following removal of TUG-891, suggesting that this issue may not ultimately preclude therapeutic agonist development at FFA4.

MOL # 87783

Materials and Methods

Materials

TUG-891 (3-(4-((4-fluoro-4'-methyl-[1,1'-biphenyl]-2-yl)methoxy)phenyl)-propanoic acid) was synthesized as described previously (Shimpukade et al., 2012). NCG21 ((4-{4-[2-(phenyl-2-pyridinylamino)ethoxy]phenyl}butyric acid)) was synthesized based on the protocol described by Suzuki et al. (Suzuki et al., 2008). TUG-905 (3-(2-fluoro-4-(((2'-methyl-4'-(3-(methylsulfonyl)propoxy)-[1,1'-biphenyl]-3-yl)methyl)amino)-phenyl)propanoic acid) was synthesized as described by Christiansen et al. (Christiansen et al., 2012). GW9508 (4-[[3-phenoxyphenyl)methyl]amino]benzenepropanoic acid) was purchased from Sigma Aldrich (Poole, UK), and GW1100 (4-[5-[(2-ethoxy-5-pyrimidinyl)methyl]-2-[[4-(4-fluorophenyl)methyl]thio]-4-oxo-1(4H)-pyrimidinyl]-benzoic acid, ethyl ester) was obtained from Cayman Chemical. YM-254890 (Takasaki et al., 2004) was the kind gift of Astellas Pharma Inc (Osaka, Japan) and Iressa (N-(3-chloro-4-fluoro-phenyl)-7-methoxy-6-(3-morpholin-4-ylpropoxy)quinazolin-4-amine) was obtained from Tocris Biosciences. Tissue culture reagents were from Life Technologies Inc. (Paisley, UK). Molecular biology enzymes and reagents were from Promega (Southampton, UK). The radiochemical [³H]deoxyglucose was from PerkinElmer Life and Analytical Sciences (Beaconsfield, Buckinghamshire, UK). All other experimental reagents were from Sigma Aldrich (Poole, UK).

Plasmids and mutagenesis

All plasmids used encoded human or mouse FFA1 or FFA4 (short isoform) receptors with enhanced yellow fluorescent protein (eYFP) fused to their C terminal and incorporating a N terminal FLAG epitope tag (FFA4 constructs only) in the pcDNA5 FRT/TO expression vector and were described previously (Smith et al., 2009; Christiansen et al., 2012; Shimpukade et al., 2012). To generate the hFFA4 construct containing a C-terminal HA epitope tag the FFA4 sequence was amplified by PCR using the primers (F- TTTTAAGCTTGCCACCATGTCCCCTGAATGCGC and R- TTTTGGATCCTTAAGCGTAATCTGGAACATCGTATGGGTAGCCAGAAATAATCGACAAGTCA), which incorporate the HA tag sequence followed by a stop codon immediately following the last

MOL # 87783

residue of FFA4. Individual point mutations, R99Q and R178Q were introduced into the FLAG-hFFA4-eYFP plasmid using the QuickChange method (Stratagene).

Cell culture, transfection and stable cell lines

In experiments utilizing transient heterologous expression we employed HEK293T cells. These were maintained in Dulbecco's Modified Eagle's Medium (DMEM) supplemented with 10% heat inactivated FBS at 37°C and 5% CO₂. Transfections were carried out with polyethylenimine and experiments conducted 48h post-transfection. In experiments using stable heterologous expression, the Flp-InTM T-RExTM system (Life Technologies Inc.) was used to generate 293 cells with doxycycline-inducible expression of the receptor of interest. All experiments carried out using these cells were conducted after 24 h treatment with 100 ng/ml doxycycline to induce receptor expression. Receptor phosphorylation experiments were carried out on CHO Flp-InTM cells stably transfected with FFA4-HA and cultured in HAM F-12 + Glutamax (Life Technologies Inc) containing 10% heat inactivated FBS, 50 units/ml of penicillin, 50 µg/ml streptomycin and 400ug/ml hygromycin b. Cells were maintained at 37°C with 5% CO₂.

In experiments where siRNA was used to knockdown β-arrestin-2 expression, FFA4 Flp-InTM T-RExTM were seeded at 25000 cells/well in 96 well plates 24 hours prior to transfecting with a pool of 4 either non-targeting or β-arrestin-2 specific siRNA oligonucleotides (Thermo Fisher Scientific) using the lipofectamine 2000 transfection reagent. Cells were transfected with a second round of siRNA 24 hour later, treated with doxycycline to induce FFA4 expression (100 ng/ml), and incubated 24 h prior to use in experiments. Successful knockdown of β-arrestin-2 mRNA was confirmed by RT-PCR using forward: GAGCCCTAACTGCAAGCTCA and reverse: AGTGTGACGGAGCATGGAAG primers.

For experiments using differentiated mouse adipocytes, 3T3-L1 fibroblasts were maintained and differentiated as described previously (Hudson et al., 2013a). Murine STC-1 and GLUTag enteroendocrine cells were maintained in DMEM supplemented with 10% heat inactivated FBS and

MOL # 87783

maintained at 37°C and 5% CO₂. For experiments, cells were plated in 24-well plates and cultured for at least 24 h before initiating GLP-1 secretion experiments. RAW 264.7 mouse macrophages were cultured in DMEM supplemented with 10% heat inactivated FBS and maintained at 37°C and 5% CO₂ and plated in 96-well plates for TNF secretion experiments. HT29 human adenocarcinoma cells were maintained in McCoy's 5A medium supplemented with 10% heat inactivated FBS and maintained at 37°C and 5% CO₂. FFA4 expression in HT29 cells was confirmed by RT-PCR utilizing primers: (F- 5'-CGCGACCAGGAAATTTTCGATT-3'; R- 5'-GTGAGCCTCTTCCTTGATGC-3') that spanned the 3rd intracellular loop region allowing for the separate detection of the short (167 bp product) and long (215 bp product) isoforms of human FFA4.

Signaling assays to assess FFA4 function

β-arrestin-1 and -2 recruitment to FFA1 or FFA4 was assessed in transiently transfected HEK293T cells after 5 min of ligand treatment using the previously described bioluminescence resonance energy transfer protocol (Shimpukade et al., 2012). Ca²⁺ mobilization experiments were carried out using Flp-InTM T-RExTM stable-inducible cell lines or HT-29 cells according to the previously described protocol (Hudson et al., 2012a). In these experiments intracellular Ca²⁺ was monitored for 90s following ligand treatment and the measured response was taken as the peak signal over this time course. Extracellular signal regulated kinase 1/2 (ERK) phosphorylation was examined in Flp-InTM T-RExTM cell lines, or in HT-29 cells following 5 min of ligand treatment (unless otherwise indicated) using a previously described protocol (Hudson et al., 2012a).

Visualization of FFA4 internalization

Human FFA4-eYFP Flp-InTM T-RExTM cells were cultured on poly-D-lysine coated glass coverslips and cultured for 24 h before treatment with doxycycline (100 ng/ml) to induce receptor expression. Live cells were then imaged using a Zeiss VivaTome spinning disk confocal microscopy

MOL # 87783

system. Images were taken prior to the addition of ligand, and every 5 min following ligand addition for a total of 45 min.

High content imaging quantitative internalization assay and cell surface ELISA

Human FFA4-eYFP Flp-InTM T-RExTM cells were plated 75000 cells per well in black with clear bottom 96-well plates. Cells were allowed to adhere for 3-6 h before the addition of doxycycline (100 ng/ml) to induce receptor expression. After an overnight incubation, culture medium was replaced with serum-free DMEM containing the ligand to be assayed. Cells were incubated at 37°C for the times indicated before fixation with 4% paraformaldehyde. After washing with PBS, cells were stained for 30 min with Hoechst 33342, washed again and plates imaged using a Cellomics Arrayscan II high content plate imager. Images were processed to identify internalized eYFP, which was then normalized to cell number based on nuclei identified by Hoechst staining to obtain a quantitative measure of hFFA4-eYFP internalization.

After imaging the plate, if FFA4 cell surface expression was also to be measured, the fixed cells were first incubated in phosphate buffered saline (PBS) containing 5% bovine serum albumin (BSA) to block non-specific binding sites (30 min at room temperature), followed by incubation with an anti-FLAG monoclonal primary antibody (30 min at room temperature), and finally with an anti-mouse horseradish peroxidase conjugated secondary antibody (30 min at room temperature). Cells were washed three times with PBS before measuring Hoechst fluorescence using a PolarStar Omega plate reader (BMG Labtech). After washing a final time with PBS, and incubating with 3,3',5,5'-tetramethylbenzidine horseradish peroxidase substrate in the dark at room temperature, the absorbance at 620 nm was measured on a PolarStar Omega plate reader. To calculate surface expression, the 620 nm absorbance corrected for cell number based on Hoechst fluorescence was expressed as a percentage of the control wild type FFA4 signal.

FFA4 phosphorylation and phosphopeptide mapping

MOL # 87783

CHO cells which stably and constitutively expressed the C-terminal HA epitope tagged FFA4 were generated. Cells were plated in 6 wells at 200,000 cells per well 24 hours prior to experimentation. For phosphorylation experiments, cells were washed 3 times with Krebs/HEPES buffer without phosphate (118 mM NaCl, 1.3 mM CaCl₂, 4.3 mM KCl, 1.17 MgSO₄, 4.17 mM NaHCO₃, 11.7 mM glucose, 10 mM HEPES [pH 7.4]) and incubated in this buffer containing 100µCi/ml ³²P orthophosphate for 1 hour at 37°C. Cells were stimulated for 5 minutes with test compounds and immediately lysed by addition of buffer containing 20 mM Tris pH 7.4, 150 mM NaCl, 3 mM EDTA, 1% NP-40, 0.5% Na deoxycholate. FFA4 was immunoprecipitated from the cleared lysates using Anti-HA Affinity Matrix (Roche Diagnostics). The washed immunoprecipitates were separated by SDS-PAGE on 10% gels which were dried and radioactive bands were revealed using autoradiography film. The films were scanned and bands quantified using alphascreen software (Alpha Innotech, San Leandro, CA).

For phosphopeptide mapping experiments, ³²P labeled FFA4 immunoprecipitates were transferred to PVDF and the band corresponding to FFA4 excised and blocked in 0.5 % polyvinylpyrrolidone K30 (PVP) in 0.6 % acetic acid at 37°C for 30 min. Tryptic peptides were generated by incubating the membrane with 1 µg sequencing grade trypsin (Promega) overnight. The resulting supernatant was dried and re-suspended in loading buffer (88 % formic acid:acetic acid:water 25:78:897 (v/v/v) pH 1.9). Peptides were applied to a 20 x 20 cm cellulose thin layer chromatography (TLC) plate and separated by electrophoresis for 30 min at 2000 V followed by ascending chromatography in isobutyric acid chromatography buffer (isobutyric acid:n-butanol:pyridine:acetic acid:water 1250:38:96:58:558 (v/v/v/v/v)). The dried plate was exposed to a storage phosphor screen for 10 days after which radioactivity was visualized using a Storm 820 Imager (Amersham Biosciences).

Single cell calcium imaging

Human FFA4-eYFP Flp-InTM T-RExTM cells were cultured on poly-D-lysine coated glass coverslips for 24 h prior to the addition of doxycycline (100 ng/ml) to induce receptor expression. Single cell Ca²⁺ measurements were then carried out as described previously (Stoddart et al., 2008b).

MOL # 87783

GLP-1 secretion from enteroendocrine cell lines

STC-1 or GLUTag cells were washed with HBSS supplemented with 20 mM HEPES before the addition of test compound in HBSS/HEPES containing the DPPIV inhibitor KR-62436 (2.5 μ M) to prevent peptidase activity and the hydrolysis of GLP-1. Cells were incubated at 37°C for 1 h before cell supernatants were collected in microcentrifuge tubes. Supernatants were then centrifuged to eliminate any cellular debris and assayed for GLP-1 concentration using an active GLP-1 ELISA kit (Millipore).

[³H]Deoxyglucose uptake assay in differentiated 3T3-L1 adipocytes

On the day of the assay differentiated 3T3-L1 adipocytes were washed once then incubated with serum-free DMEM for 2 h at 37°C. Cells were transferred to a hot plate maintained at 37°C and then washed three times with Krebs-Ringer-Phosphate buffer (128 mM NaCl, 1.25 mM CaCl₂, 4.7 mM KCl, 5.0 mM NaH₂PO₄, 1.25 mM MgSO₄) (KRP). Cells were then incubated for 30 min in KRP containing either the ligand to be assayed or insulin prior to the addition of a [³H]deoxyglucose/deoxyglucose solution yielding final assay concentrations of 1 μ Ci of [³H]deoxyglucose and 50 μ M deoxyglucose. After incubating 5 min to allow for [³H]deoxyglucose uptake, the KRB buffer was removed quickly by inverting before the plates were submerged sequentially 3 times in ice cold PBS to stop the reaction and wash the cells. Plates were then allowed to dry for at least 30 min before cells were solubilized overnight with 1% Triton X-100. Solubilized material was then collected and [³H] levels assessed by liquid scintillation spectrometry.

TNF secretion from RAW264.7 macrophages

RAW264.7 macrophages were plated 25000 cells per well in 96-well plates and cultured overnight. Medium was removed and replaced with fresh serum-free medium supplemented with 0.01% BSA, and containing the compound to be tested. After a 1 h incubation lipopolysaccharide (LPS) was

MOL # 87783

added (100 ng/ml) to stimulate TNF release. Cells were maintained for 6 h at 37°C before supernatants were collected and assayed for TNF in low volume white 384 well plates using a mouse TNF AlphaLISA assay kit (PerkinElmer).

Data analysis and curve fitting

Data presented represent mean \pm standard error of at least three independent experiments. Data analysis and curve fitting was carried out using the Graphpad Prism software package v5.0b. Concentration-response data were plotted on a log axis, where the untreated vehicle control condition was plotted at one log unit lower than the lowest test concentration of ligand and fitted to three-parameter sigmoidal concentration-response curves. Statistical analysis was carried out using standard t-tests or 1-way analysis of variance followed by Tukey's post-hoc test tests as appropriate.

MOL # 87783

Results

TUG-891 is a potent agonist of FFA4

Post-activation assays were established to examine the ability of TUG-891 and various other ligands to activate FFA4. Initially, we compared the actions of TUG-891 (**Figure 1A**) with key, previously described, ligands with reported agonist activity at FFA4. These included the endogenous fatty acid agonist α -linolenic acid (aLA) (**Figure 1A**); the FFA1 selective agonist GW9508 (**Figure 1A**) (Briscoe et al., 2006), which has been used in the absence of other ligands to study FFA4 function; and NCG21 (**Figure 1A**), the most selective synthetic FFA4 agonist previously described in the academic literature (Suzuki et al., 2008). FFA4 has been shown to couple to $G\alpha_{q/11}$ -initiated signal transduction pathways and, as such, we first assessed the activity of these four compounds in Ca^{2+} mobilization assays employing Flp-InTM T-RExTM 293 cells that had been engineered to express human FFA4 (hFFA4) only upon treatment with the antibiotic doxycycline. All four ligands produced concentration-dependent increases in intracellular Ca^{2+} with TUG-891 being the most potent; approximately 7-fold more potent than GW9508 and 50-fold more potent than aLA and NCG21 (**Figure 1B** and **Table 1**). These responses to each ligand reflected activation of FFA4, as no responses were observed in cells that had not been treated with doxycycline to induce expression of hFFA4 (data not shown).

In addition to promoting signaling via the $G_{q/11}$ G proteins FFA4 has also been reported to couple to G protein-independent, β -arrestin-2-mediated pathways (Oh et al., 2010; Shimpukade et al., 2012). We next examined, therefore, the potency of the same ligands in a bioluminescence resonance energy transfer (BRET)-based β -arrestin-2 recruitment assay utilizing HEK293T cells transiently co-transfected with an eYFP-tagged form of hFFA4 and a *Renilla* luciferase-tagged form of β -arrestin-2 (**Figure 1C**). All four compounds again produced concentration-dependent responses with the rank-order of potency being similar to that observed in the Ca^{2+} assays. TUG-891 was the most potent, and was approximately 10-fold more potent than GW9508, 35-fold more than NCG21, and 80-fold more potent than aLA (**Table 1**). We also established a similar BRET assay to examine β -arrestin-1 recruitment to FFA4. Each ligand was

MOL # 87783

able to recruit β -arrestin-1 with the same rank-order, although slightly reduced potency, compared with β -arrestin-2 recruitment (**Table 1**).

FFA4 activation has also been linked to increased phosphorylation of the extracellular signal-regulated kinases (ERK) 1 and 2 (Suzuki et al., 2008). Activation of ERK can be induced by either G protein-dependent or-independent pathways (Shenoy et al., 2006). In this assay, again utilizing hFFA4-inducible Flp-InTM T-RExTM 293 cells, only TUG-891 and GW9508 produced activation in a clear, concentration-dependent manner whilst aLA and NCG21 only increased ERK phosphorylation at the highest concentrations that could be employed (**Figure 1D**). Interestingly, although the rank-order of potency observed in the other assays of TUG-891 > GW9508 > NCG21 \approx aLA remained intact in the ERK assay, the potency of each compound was significantly reduced ($p < 0.001$) in this assay compared with the values obtained from either Ca²⁺ mobilization or β -arrestin-2 interaction studies (**Table 1**). Construction of ‘bias-plots’ (Gregory et al., 2010) comparing responses to equivalent concentrations of ligand between each of the three assays (**Figures 1E-G**) clearly demonstrated an inherent bias in FFA4 signaling towards Ca²⁺ and β -arrestin-2 recruitment over ERK phosphorylation. However, as the bias-plot profiles were similar for all four ligands in each assay comparison, these data suggest that each ligand is likely to activate the receptor in a similar manner.

FFA4 stimulates ERK phosphorylation primarily through G_{q/11}

GPCRs are known to stimulate ERK phosphorylation through a number of different pathways. We therefore explored the mechanism(s) allowing FFA4 mediated ERK activation. Time course studies (**Figure 2A**) indicated that aLA and TUG-891 produced similar kinetic pERK response profiles. An initial peak response was observed within 2.5 min, followed by a rapid decrease in pERK until 10 min of ligand treatment when the pERK levels plateaued. This was followed by a gradual decline in pERK up to 60 min of ligand treatment, when levels had returned close to basal. By contrast treatment with 10 % (v/v)

MOL # 87783

FBS resulted in a slower pERK response, reaching a peak at 5 min that decreased much more rapidly, returning to basal levels within 10 min. We next examined whether the pERK response was $G_{q/11}$ mediated and/or involved transactivation of the Epidermal Growth Factor (EGF) receptor, as shown for FFA4 in Caco-2 adenocarcinoma cells (Mobraten et al. 2013). The $G_{q/11}$ inhibitor YM-254890 significantly inhibited but did not eliminate the 5 min response to either aLA ($p < 0.05$; 52% reduction) or TUG-891 ($p < 0.001$; 65% reduction) (**Figure 2B**). In contrast YM-254890 did not inhibit the 5 min response produced by FBS ($p > 0.05$) (**Figure 2B**). The EGF receptor inhibitor, 'Iressa', had no effect on the 5 min response to any of the ligands. We also assessed any effects of YM-254890 or Iressa on the pERK plateau observed after 15 min of treatment with either aLA or TUG-891 (**Figure 2C**). At this time point YM-254890 also significantly reduced the pERK response to both aLA and TUG-891 ($p < 0.001$), reductions of $60 \pm 9\%$ and $70 \pm 7\%$ respectively. Now, however, Iressa also partially inhibited the pERK responses by $33 \pm 7\%$ to aLA ($p < 0.001$) and by $31 \pm 12\%$ to TUG-891 ($p < 0.05$). Moreover, combined treatment with both YM-254890 and Iressa entirely eliminated pERK activation by both ligands at 15 min. To confirm that Iressa and YM-254890 were able to effectively block EGF receptor- and $G_{q/11}$ -mediated signaling respectively at the concentrations used, we demonstrated that Iressa completely blocked EGF-mediated ERK phosphorylation (**Figure 2D**) and that YM-254890 completely eliminated the TUG-891 mediated elevation of $[Ca^{2+}]$ in these cells (**Figure 2E**).

Because neither YM-254890 nor Iressa were able to fully block FFA4-mediated ERK phosphorylation at the peak time point, this suggests other pathways are involved. We, therefore, also examined whether a portion of this FFA4 pERK response might be mediated by β -arrestin-2. siRNA was used to knockdown expression of β -arrestin-2 in the FFA4-eYFP Flp-InTM T-RExTM 293 cell line and pERK induction by aLA, TUG-891 and FBS assessed after either 5 min (**Figure 2F**). In each case the pERK response was unaffected, despite the fact that the siRNA did greatly reduce β -arrestin-2 mRNA levels. To confirm that we had achieved functional knockdown of β -arrestin-2 we observed TUG-891-mediated internalization of FFA4-eYFP in control or β -arrestin-2 siRNA transfected cells by fluorescent

MOL # 87783

microscopy (**Figure 2G**). An apparent reduction in FFA4-internalization in β -arrestin-2 siRNA transfected cells was observed, and quantitative measure of this indicated that the siRNA resulted in a $70 \pm 9\%$ reduction in TUG-891 mediated internalization of FFA4 (**Figure 2H**). These results indicate a lack of involvement of β -arrestin-2 in FFA4-mediated ERK phosphorylation in these cells. Instead, FFA4 rapidly activates ERK primarily through $G_{q/11}$, while the more sustained pERK response involves a combination of $G_{q/11}$ and EGF transactivation pathways.

TUG-891 stimulates rapid internalization, phosphorylation and desensitization of FFA4

Like many GPCRs, following ligand activation, FFA4 can be internalized away from the plasma membrane (Hirasawa et al., 2005; Watson et al., 2012). In the hFFA4 Flp-InTM T-RExTM 293 cell line internalization of hFFA4-eYFP was assessed by confocal microscopy. Before ligand treatment hFFA4-eYFP was located primarily at the cell surface, however, within 10 min of the addition of 100 μ M aLA an increase in intracellular hFFA4-eYFP expression was observed, with a punctate distribution (**Figure 3A**). The amount of internalized hFFA4-eYFP increased over time and within the 45 min incubation period employed there was very little hFFA4-eYFP that could be observed at the cell surface. 10 μ M TUG-891 produced a similar pattern of internalization (**Figure 3B**). To quantify these effects we employed a high content imaging assay that measures the intensity of eYFP fluorescence within internal cellular compartments, an approach that has been used previously to quantitatively assess GPR120 internalization (Fukunaga et al. 2006; Watson et al. 2012). This assay demonstrated that the amount of internalized receptor increased in a quasi-linear fashion for both ligands, and with similar kinetics, reaching a maximum level within 40 min (**Figure 3C**). Interestingly, although the potency of TUG-891 in this assay was similar to that of the BRET β -arrestin-2 and Ca^{2+} assays (**Table 1**), the rank-order of potency for the 4 ligands was distinct: TUG-891 > NCG21 > GW9508 > aLA (**Figure 3D**).

MOL # 87783

In addition to being internalized away from the cell surface, many GPCRs become phosphorylated rapidly after ligand activation to both promote interactions with β -arrestins and as a means to induce desensitization. Previous studies have demonstrated phosphorylation of FFA4 in response to fatty acid ligands (Burns and Moniri, 2010). We confirmed that as well as aLA, TUG-891 was able to promote phosphorylation of hFFA4 (**Figure 3E and 3F**). Furthermore, aLA and TUG-891 appeared to stimulate phosphorylation at the same sites as indicated by the fact that the patterns of phospho-peptides generated from tryptically digested hFFA4 were the same when resolved by 2D chromatography (**Figure 3G**). As an extension we explored whether TUG-891 promoted desensitization of the receptor signaling response. Single cell Ca^{2+} measurements allow repeated ligand treatment and washout (**Figure 3H**). Treatment with TUG-891 (3 μM) for 2 min resulted in a rapid increase in intracellular Ca^{2+} , which returned to baseline after the ligand was removed. A second 2 min treatment with TUG-891 resulted in a Ca^{2+} response that was only $42 \pm 12\%$ of the original, while a third treatment resulted in a further reduction to only $34 \pm 11\%$ of the original response. This did not reflect a simple run-down of capacity as when cells were stimulated subsequently with ATP they were still competent to produce a full Ca^{2+} response.

FFA4 rapidly recycles back to the cell surface and restores responsiveness after removal of TUG-891

We next examined whether FFA4 can recycle and rapidly restore responsiveness after washout of TUG-891. After inducing expression in hFFA4 Flp-InTM T-RExTM 293 cells, doxycycline was removed to cease *de novo* FFA4 production. Cells were then treated with either vehicle (0.01% DMSO), or TUG-891 (10 μM) for 45 min, washed 4 times with HBSS containing 0.5% BSA to remove TUG-891, then either fixed immediately or allowed to recover for 60 min and fixed before imaging by fluorescence microscopy. Recovery of hFFA4-eYFP expression at the cell surface appeared to be largely complete within this time period (**Figure 4A**). Such visual studies do not provide direct quantification. We therefore measured in parallel total hFFA4-eYFP expression (measuring total eYFP), cell surface hFFA4-

MOL # 87783

eYFP expression (using cell surface ELISA against the N-terminal FLAG epitope present in the hFFA4-eYFP construct), and internalized FFA4-eYFP (employing high content imaging) in the same samples after treatment with TUG-891 to stimulate internalization. Cells were washed 4 times with HBSS containing 0.5% BSA to remove the TUG-891, and fixed at 10 min recovery intervals for up to 1 h (**Figures 4B-D**). There was no measurable receptor degradation, as the total receptor-eYFP levels remained constant (**Figure 4B**). Surface expression levels recovered, from a significant ($p < 0.001$) $75 \pm 8\%$ decrease in FFA4-eYFP induced by treatment with TUG-891, in a time-dependent manner such that by 60 min they had returned to $78 \pm 10\%$ of the vehicle treated control. To confirm this increase in cell surface expression resulted from internalized receptors being trafficked back to the cell surface, the amount of internalized receptor measured in the high content imaging assay demonstrated a parallel decrease in internal receptor with increasing recovery times (**Figure 4D**). We also assessed if signaling responses to TUG-891 recovered as a result. Following treatment of hFFA4 Flp-InTM T-RExTM 293 cells with either vehicle or TUG-891 (10 μ M) for 45 min and washing, Ca²⁺ responses to TUG-891 were assessed at 10 min intervals (**Figure 4E**). Although desensitization resulted in a complete loss of TUG-891 response, by 10 and 20 min recovery the cells had regained an acute response to TUG-891. At these time points the recovered response was sub-maximal being only $61 \pm 5\%$ ($p < 0.001$) and $83 \pm 4\%$ ($p < 0.05$) respectively of controls. However, between 30 and 60 min following removal of TUG-891, recovery of Ca²⁺ response to was fully resensitized, showing no difference ($p > 0.05$) from the control (**Figure 4E**).

To compare in detail the relationship between cell surface expression recovery, reduction in internalized receptor, and resensitization of the Ca²⁺ signaling response, we generated correlation plots for each of these parameters (**Figures 4F-H**). As expected, there was a negative linear correlation (-0.94 ; $p < 0.01$) when comparing surface expression and internalized receptor (**Figure 4F**). Interestingly, although there was a linear relationship between FFA4 surface expression and Ca²⁺ response, this was only true up to 50% cell surface expression, after which there was no further increase in Ca²⁺ response

MOL # 87783

(**Figure 4G**). Similarly, although there was a negative relationship between the amount of internalized receptor and the Ca^{2+} response, this again was only linear between ~50 and 100% internalized receptor, as further reduction in the level of internalized receptor had little affect the Ca^{2+} response. Together, these findings indicate that only approximately 50% surface expression of hFFA4 is required to achieve the maximal Ca^{2+} signal in these cells and demonstrates a significant level of receptor reserve.

TUG-891 is an orthosteric FFA4 agonist

Binding of fatty acid ligands to the three structurally related members of the FFA receptor family, FFA1-3, has been shown to involve ionic interactions between the carboxylate of the fatty acid ligand and conserved, positively charged arginine residues near the extracellular end of transmembrane domains (TMDs) V and VII (Tikhonova et al., 2007; Stoddart et al., 2008b). These residues are not conserved in FFA4. However, there are two arginine residues close to the extracellular face of FFA4, R99 in TMDII and R178 in TMDIV; and several recent modeling an/or mutational studies have suggested that R99 in particular is important for ligand binding to FFA4 (Suzuki et al., 2008; Sun et al., 2010; Watson et al., 2012). When assessed in the β -arrestin-2 BRET interaction assay aLA was unable to activate an R99Q mutant form of hFFA4 but the activity and potency of this ligand was unaffected at an R178Q hFFA4 mutant (**Figure 5A**). TUG-891 displayed the same pattern, losing function at R99Q hFFA4 but not at R178Q hFFA4 (**Figure 5B**), suggesting that R99 is critical to the binding of both endogenous fatty acids and TUG-891. To define that the lack of function observed at R99Q hFFA4 did not simply reflect lack of expression of the mutant, we measured the relative expression levels of the wild type and mutant hFFA4 constructs both at the cell surface by ELISA using an antibody directed against the N-terminal FLAG epitope tag present in the constructs, and total expression assessed by eYFP fluorescence (**Figure 5C**). These experiments demonstrated that R99Q hFFA4 did show significantly less ($p < 0.001$) cell surface ($29 \pm 4\%$ of wild type) and total ($60 \pm 1\%$ of wild type) expression; while R178Q hFFA4 had similar total

MOL # 87783

expression to wild type and only modestly reduced cell surface expression ($75 \pm 5\%$ of wild type). Hence, although neither mutant was delivered to the cell surface as efficiently as wild type hFFA4, both are able to reach the cell surface in some level, suggesting that the complete lack of ligand function at R99Q hFFA4 is consistent with this residue being involved directly in ligand binding and function.

TUG-891 is a selective agonist for hFFA4

Despite limited homology between the two LCFA receptors, identifying ligands that are markedly selective for FFA4 over FFA1 has been challenging. We examined, therefore, the selectivity of TUG-891 at hFFA4 compared to hFFA1 using the β -arrestin-2 recruitment assay (**Figures 6A-6D**). TUG-891 was markedly selective for hFFA4, being some 288-fold more potent at hFFA4 ($pEC_{50} = 7.22 \pm 0.06$) than hFFA1 ($pEC_{50} = 4.76 \pm 0.29$). By contrast the fatty acid agonist aLA lacked selectivity, being only 3-fold more potent at hFFA4 ($pEC_{50} = 5.11 \pm 0.05$) than at hFFA1 ($pEC_{50} = 4.63 \pm 0.15$). As anticipated from previous work (Briscoe et al., 2006), GW9508 was selective for FFA1 (19-fold; pEC_{50} 's of 6.03 ± 0.03 and 7.32 ± 0.20 at hFFA4 and hFFA1 respectively) although displaying good potency at hFFA4, and NCG21 displayed modest, 12-fold selectivity for hFFA4 ($pEC_{50} = 5.72 \pm 0.08$) over hFFA1 (4.63 ± 0.15). To examine the two apparently most FFA4 selective compounds, NCG21 and TUG-891, in alternate signaling pathways we also compared the potency of these compounds in Ca^{2+} assays for both hFFA4 and hFFA1 (**Figures 6E and 6F**). In these assays NCG21 again showed modest 8-fold selectivity for hFFA4 ($pEC_{50} = 5.04 \pm 0.10$) over hFFA1 ($pEC_{50} = 4.13 \pm 0.13$), while TUG-891 was again substantially more selective for FFA4 (52-fold; pEC_{50} values of 7.02 ± 0.09 and 5.30 ± 0.04 for hFFA4 and hFFA1 respectively). Taken together, these experiments indicate that TUG-891 is the most potent and selective agonist of hFFA4 currently described and is, therefore, likely to represent the most suitable ligand to explore the function of FFA4 in native human systems.

TUG-891 produces similar signaling responses in HT29 cells that express hFFA4 endogenously

MOL # 87783

We next assessed if TUG-891 could be used to examine hFFA4 function in human derived cells that endogenously express the receptor. Two different isoforms of FFA4 have been described in human, differing by a 16 amino acid insertion in the third intracellular loop (Watson et al., 2012). We therefore designed RT-PCR primers anticipated to yield different sized PCR products from the short and the long isoforms, and used these to assess FFA4 transcript expression in the human HT29 adenocarcinoma cell line. A single fragment, corresponding to the short isoform, was identified (**Figure 7A**), indicating that HT29 cells express the short, but not long isoform of FFA4. Both aLA and TUG-891 produced concentration-dependent increases in intracellular Ca^{2+} (**Figure 7B**) in these cells with TUG-891 substantially more potent than aLA (pEC₅₀ values of 5.35 ± 0.10 and 4.48 ± 0.16 respectively). However, the potency of each ligand was substantially lower than in Ca^{2+} assays performed with Flp-InTM T-RExTM 293 cells heterologously expressing hFFA4 (**Table 1**). Similar experiments explored ERK phosphorylation in response to aLA or TUG-891 in HT29 cells (**Figure 7C**). Concentration-dependent responses were again obtained for both aLA (pEC₅₀ = 3.46 ± 0.27) and TUG-891 (pEC₅₀ = 5.13 ± 0.12). As in the hFFA4 Flp-InTM T-RExTM 293 cells, the potencies of these two ligands in the pERK assay were lower than in the Ca^{2+} assay, suggesting that despite the reduced overall potency in these cells the pharmacology of aLA and TUG-891 is similar in the two systems.

TUG-891 is also a potent agonist of mFFA4

We have previously noted marked differences in ligand potency between species orthologs of other members of the FFA family (Hudson et al., 2012a; 2012b; 2013a). We examined, therefore, the activity and potency of TUG-891 and other ligands at the mouse ortholog of FFA4 (mFFA4). In the β -arrestin-2 recruitment assay (**Figure 8A**) the rank order of potency at mFFA4 was similar to that observed at hFFA4: with TUG-891 (pEC₅₀ = 7.77 ± 0.09) > GW9508 (pEC₅₀ = 6.54 ± 0.05) > NCG21 (pEC₅₀ = 5.77 ± 0.05) > aLA (pEC₅₀ = 5.07 ± 0.07). We next assessed whether TUG-891 also displayed a similar

MOL # 87783

degree of selectivity for mFFA4 over mFFA1 in the β -arrestin-2 assay (**Figure 8B**). TUG-891 displayed greater potency at mFFA1 ($pEC_{50} = 5.92 \pm 0.16$) than observed at hFFA1 (**Figure 6**; $pEC_{50} = 4.76 \pm 0.29$). Despite this, TUG-891 still displayed a substantial 61-fold selectivity for mFFA4 over mFFA1 in this assay. As we had observed potency and selectivity differences for TUG-891 at hFFA4 between different assays, we also examined the selectivity of TUG-891 for mFFA4 over mFFA1 in Ca^{2+} mobilization assays (**Figure 8C**). Here TUG-891 was found to have reduced potency at mFFA4 ($pEC_{50} = 6.89 \pm 0.04$). Moreover, TUG-891 displayed somewhat greater potency at mFFA1 ($pEC_{50} = 6.41 \pm 0.08$). As a result, the selectivity of TUG-891 for mFFA4 over mFFA1 was reduced to only 3-fold in the Ca^{2+} assay.

The relatively low selectivity for TUG-891 at the mouse orthologs in ability to elevate Ca^{2+} suggests that using this compound in murine-derived cells that co-express both FFA4 and FFA1 is likely to limit its use in defining specific functions of each receptor. Despite the availability of a substantial pharmacological armory of FFA1 ligands, including antagonists as well as agonists, there is little information available on possible selectivity of these compounds at mFFA1 versus mFFA4. Therefore, to identify ligands that would be useful to employ in concert with TUG-891 to define mFFA1 versus mFFA4 function we assessed an FFA1 agonist, TUG-905 (Christiansen et al., 2012), which we have previously noted to be particularly potent at mFFA1. In Ca^{2+} assays employing Flp-InTM T-RExTM cells TUG-905 was indeed a potent agonist of mFFA1 ($pEC_{50} = 7.03 \pm 0.06$) (**Figure 8D**) but produced little response at mFFA4 at concentrations up to 100 μ M. TUG-905 is, therefore, at least 1000-fold selective for mFFA1 over mFFA4 and may be used to define function of FFA1 in murine-derived cells and tissues. We also explored the ability of GW1100 (Briscoe et al., 2006), a FFA1 antagonist which we confirmed to have no effect at either hFFA4 or mFFA4 (data not shown) to inhibit signals in response to each of TUG-905, TUG-891 and aLA at mFFA1. In Ca^{2+} mobilization assays GW1100 inhibited the responses to each ligand in a concentration-dependent manner with 10 μ M GW1100 completely blocking each response (**Figure 8E**). Together, these findings indicated that combinations of TUG-891, TUG-905 and GW1100

MOL # 87783

would allow definition of the contributions of mFFA4 and mFFA1 in mouse cells and tissues that co-express the two FFA receptors.

TUG-891 stimulates GLP-1 secretion in both STC-1 and GLUTag mouse enteroendocrine cell lines

It has previously been suggested that fatty acids stimulate secretion of GLP-1 from enteroendocrine cells through activation of FFA4 (Hirasawa et al., 2005). We, therefore, re-examined this question by initially defining if TUG-891 was able to stimulate GLP-1 secretion from two different, mouse derived enteroendocrine cell lines, STC-1 and GLUTag. Expression of both mFFA1 and mFFA4 was shown in each cell line by RT-PCR (**Figure 9A**). In STC-1 cells a robust, statistically significant ($p < 0.001$) increase in GLP-1 secretion was produced upon addition of either aLA (100 μM) or TUG-891 (30 μM) (**Figure 9B**). By contrast only a small increase, that did not reach statistical significance, was observed in response to TUG-905 (10 μM). The FFA1 antagonist GW1100 (10 μM) was without effect on aLA-induced GLP-1 secretion, and although GW1100 significantly reduced the response to TUG-891 ($p < 0.01$), it did so by only 26% (**Figure 9B**). GW1100 also blocked the apparent small increase in GLP-1 secretion produced by TUG-905. When similar experiments were performed using the GLUTag cell line highly similar patterns of GLP-1 responses were observed (**Figure 9C**). Again both aLA (100 μM ; $p < 0.001$) and TUG-891 (30 μM ; $p < 0.01$) increased GLP-1 secretion, while TUG-905 again produced a marginal response that did not reach statistical significance. Co-addition of GW1100 again failed to inhibit the aLA response, and in this case, also did not produce a significant reduction in the response to TUG-891 ($p > 0.05$). Taken together, the data from these murine enteroendocrine cell lines indicate that TUG-891 robustly stimulates GLP-1 release, primarily through activation of FFA4. However, a small component of the TUG-891 GLP-1 response does appear to be mediated by FFA1.

TUG-891 stimulates glucose uptake in differentiated 3T3-L1 adipocytes and inhibits tumor necrosis factor (TNF) secretion from RAW 264.7 macrophages

MOL # 87783

FFA4 expression has been reported previously in adipocytes and the receptor suggested to stimulate increased glucose uptake (Oh et al., 2010). When using differentiated 3T3-L1 mouse adipocytes as a model, treatment with aLA (100 μ M) produced a statistically significant ($p < 0.01$) $92 \pm 20\%$ increase in [3 H]deoxyglucose uptake by these cells (**Figure 10A**). Treatment with TUG-891 (10 μ M) also produced a significant increase ($p < 0.05$) of [3 H]deoxyglucose uptake, however, in this case only by $47 \pm 18\%$. The responses to either aLA or TUG-891 were, however, modest in comparison to the $557 \pm 164\%$ increase observed upon challenge with insulin (1 μ M) (**Figure 10A**). Despite the increases in [3 H]deoxyglucose uptake produced in response to aLA and TUG-891 being modest in extent, they were concentration-dependent with pEC_{50} s of 4.69 ± 0.28 and 5.86 ± 0.29 respectively (**Figures 10B and 10C**). Although lower than potency measures obtained in cells heterologously expressing mFFA4, these potency differences are similar to those observed between HT29 cells endogenously expressing the hFFA4 receptor and assays employing heterologously expressed hFFA4.

A further area of potential FFA4 function that has received substantial interest is that the receptor may mediate the anti-inflammatory properties of the n-3 fatty acid docosahexaenoic acid (DHA) in macrophage-like cells (Oh et al., 2010). In RAW 264.7 cells LPS treatment produced a robust increase in TNF secretion that was significantly inhibited by aLA ($29 \pm 12\%$; $p < 0.05$), TUG-891 ($30 \pm 6\%$; $p < 0.05$) and DHA ($88 \pm 4\%$), but not by TUG-905 (**Figure 10D**). These results indicate that the FFA4 agonist TUG-891 can produce an anti-inflammatory effect in these cells, however, with substantially lower efficacy than DHA. The inhibition of TNF secretion in these cells by both aLA and TUG-891 was also concentration-dependent with pIC_{50} values of 4.79 ± 0.39 and 5.86 ± 0.29 respectively (**Figures 10E and 10F**), very similar to the potencies observed for each ligand in the 3T3-L1 glucose uptake experiments.

MOL # 87783

Discussion

In recent years GPCRs of the FFA family have been receiving increasing interest for their potential use as novel therapeutic targets in the treatment of both metabolic and inflammatory conditions (Holliday et al., 2011; Hudson et al., 2011; 2013b). While the focus, to date, has been largely on FFA1, interest in FFA4 has also been steadily increasing as a target for the treatment of obesity and type 2 diabetes. In large part this reflects recent knockout, knockdown and genetic studies consistent with this receptor playing important roles in GLP-1 secretion, β -cell survival, glucose uptake and insulin sensitization, as well as producing anti-inflammatory effects (Hirasawa et al., 2005; Oh et al., 2010; Ichimura et al., 2012; Taneera et al., 2012). Despite this interest, further validation of FFA4 as a therapeutic target has been slowed by a lack of available small molecule ligands for this receptor. The recent discovery of TUG-891, described as a potent and selective agonist for FFA4 (Shimpukade et al., 2012) has begun to address this deficit and, in the current work, we have used this ligand to explore the pharmacology and function of FFA4 in various cell models either heterologously or endogenously expressing species orthologs of this receptor. The results generated demonstrate both potential, but also significant challenges that may complicate the development of FFA4 as a therapeutic target.

Comparison of TUG-891 with other currently available agonists of FFA4, including the endogenous fatty acid aLA, the FFA1 selective agonist GW9508 (Briscoe et al., 2006), and the only other previously described FFA4 synthetic agonist with a degree of selectivity, NCG21 (Suzuki et al., 2008), clearly demonstrated TUG-891 to be the most potent and selective compound for hFFA4. Importantly, the signaling pathways and responses for TUG-891 at hFFA4 were observed to be very similar to those of the endogenously generated fatty acid aLA, producing similar response kinetics, bias plot profiles and efficacies in all endpoints examined. This is consistent with TUG-891 being largely equivalent in function to aLA and, in concert with both aLA and TUG-891 lacking function at the R99Q hFFA4 mutant, with TUG-891 being an orthosteric agonist. Interestingly, bias plots comparing the function of FFA4 agonists at ERK phosphorylation, β -arrestin-2 recruitment and Ca^{2+} mobilization assays indicate

MOL # 87783

that this receptor shows a ‘natural bias’ away from the ERK pathway (Gregory et al., 2010; 2012), an observation that is further supported by the noted lower potency for aLA and TUG-891 in the pERK assay when employing human derived HT-29 cells that endogenously express FFA4. Because of this natural bias, we explored in more detail specific mechanisms allowing FFA4 mediated ERK phosphorylation and demonstrated an apparent biphasic pERK response that was dependent on both $G_{q/11}$ (early and later responses), as well as EGF receptor transactivation (late response only). While previous work has suggested FFA4 mediates a slow EGF receptor-dependent pERK response in Caco-2 adenocarcinoma cells (Mobraten et al. 2013), the rapid ERK response was not observed in these cells, suggesting FFA4 activates ERK through different pathways in different cell types. It was also interesting to note that despite the very strong interaction between FFA4 and β -arrestin-2, the ERK response in the current studies did not involve β -arrestin-2 signaling. Finally, although the rapid pERK response was reduced substantially by inhibition of $G_{q/11}$ signaling, it was not fully blocked, suggesting FFA4 couples to an as yet unknown $G_{q/11}/\beta$ -arrestin-2 independent signaling pathway(s) in these cells.

Complicating interpretation of the pharmacology of FFA4 is our observation that the measured potency of both TUG-891 and aLA was substantially lower in cells endogenously expressing the receptor compared to values observed using heterologous expression systems. While such observations often reflect variation in receptor reserve, both the β -arrestin-2 BRET and internalization assays are expected conceptually to predict the affinity of the compound as the responses are anticipated to directly reflect receptor occupancy (Hudson et al., 2011) and, therefore, would not be expected to show substantial effects of receptor reserve. However, our observation that only 50% cell surface recovery was needed to regain a full efficacy Ca^{2+} response in the FFA4 Flp-InTM T-RExTM 293 cells does suggest that a receptor reserve is present, at least when measuring Ca^{2+} in this cell line. Considering this, there is clearly a need to develop assays that can directly measure the affinity of ligands at FFA4. Although such assays have been challenging for receptors with very lipophilic ligands, several approaches have now been reported to

MOL # 87783

directly measure ligand affinity at FFA1 (Hara et al., 2009b; Bartoschek et al., 2010; Negoro et al., 2012) and may be equally suitable for studies with FFA4.

Although our work demonstrates TUG-891 to be the best available ligand for analysis of function at hFFA4, with similar signaling properties to the endogenous ligand, aLA, we also observed several issues that may complicate development of this, or other FFA4 agonists, as therapeutics. Firstly, although previous work has shown that activation of FFA4 by fatty acids stimulates both rapid phosphorylation (Burns and Moniri, 2010) and internalization (Hirasawa et al., 2005) of the receptor, the decreased Ca^{2+} responses we observed upon repeated exposure to TUG-891 suggests that receptor desensitization may present a significant challenge for FFA4. While this may present a challenge to drug development at FFA4, our observation that FFA4 does recycle back the cell surface and resensitize quickly after the removal of TUG-891 is encouraging that long term agonism of this receptor may still be therapeutically viable. Clearly, it will be important for future work to explore how these factors may affect long term FFA4 agonist treatment *in vivo*.

A second significant issue raised by this study is that the selectivity of ligands for FFA4 cannot be assumed to be equivalent across species. Most notably, although TUG-891 was more potent at mFFA4 than hFFA4 in the β -arrestin-2 assay, the opposite was true when measuring Ca^{2+} elevation. Coupled to the observation that TUG-891 was more potent at mFFA1 than hFFA1, particularly again in Ca^{2+} assays, TUG-891 is likely to be only marginally selective for mFFA4 over mFFA1, at least for end-points that reflect $\text{G}_{q/11}$ -mediated signaling. Further complicating the issue is the observation that TUG-891, and other FFA4 agonists, displayed lower potency in cell systems endogenously expressing the receptor. This suggests that the most effective means to pharmacologically define a contribution of mFFA4 in mice, or in cells derived from them where FFA1 is co-expressed, will require the use of combinations of TUG-891 alongside FFA1 antagonists. Although the development and detailed characterization of FFA4 antagonists may, in time, overcome this issue we demonstrated the clear benefit of incorporating FFA1 antagonist studies in showing that TUG-891-stimulated GLP-1 release from both the murine STC-1 and GLUTag

MOL # 87783

enteroendocrine cell lines is mediated predominantly by FFA4. However, the partial effect of the FFA1 antagonist GW1100 on the effects of TUG-891 does suggest a contribution from FFA1 as well. This is perhaps not surprising given the limited FFA4/FFA1 selectivity of TUG-891 at the mouse orthologs, and that both receptors have been linked to fatty acid stimulated GLP-1 release in the past (Hirasawa et al., 2005; Edfalk et al., 2008; Luo et al., 2012). Indeed, our findings with TUG-891 may suggest that FFA1 and FFA4 produce additive effects on GLP-1 release, consistent with the concept that a dual agonist for these two receptors may be therapeutically useful. The idea of a dual FFA1/FFA4 agonist for the treatment of type 2 diabetes is potentially very interesting given the variety of beneficial effects each receptor has been linked with (Holliday et al., 2011). In particular, the fact that FFA1 agonism is well known to enhance GSIS in β -cells and FFA4 agonism promotes survival of these same cells, makes a strong case for potentially synergistic properties of dual FFA1/FFA4 agonists on insulin secretion and β -cell maintenance. Moreover, given our observations with TUG-891 at the mouse orthologs of these receptors, this molecule may be an excellent candidate to test this hypothesis.

Although the poor selectivity of TUG-891 for FFA4 in mouse systems presents challenges, this molecule can be extremely useful for assessing FFA4 function in cells that do not express FFA1. We took advantage of this to examine the properties of TUG-891 in both differentiated 3T3-L1 adipocytes and RAW 264.7 macrophages, two cell lines previously shown to express only FFA4 (Gotoh et al. 2007; Oh et al., 2010). TUG-891 both stimulated insulin-independent glucose uptake in 3T3-L1 cells, and inhibited LPS-induced TNF secretion from RAW 264.7 cells. These observations are consistent with previous work indicating that n-3 fatty acids produce each of these effects via activation of FFA4 (Oh et al., 2010). However, it should also be noted that the magnitude of these TUG-891 responses were relatively small. For example, in glucose uptake studies TUG-891 produced a response that was only 8% of the maximal insulin response, while inhibition of TNF production by TUG-891, although of similar extent to that produced by aLA, was only 34% of that observed with the n-3 fatty acid DHA. The fact that TUG-891 does not produce as large an effect as DHA in regulation of inflammatory mediator release perhaps

MOL # 87783

indicates that the relatively high concentration of DHA required results in at least some of its anti-inflammatory effect being produced through mechanisms other than FFA4 activation including, for example, previously described pathways involving COX2 or PPAR γ (Li et al., 2005; Groeger et al., 2010). Together, the relatively low efficacy of TUG-891 in both glucose uptake and anti-inflammatory assays does raise questions as to whether this, or other FFA4 agonists, will produce therapeutically relevant responses and whether this may be related to our observations that FFA4 is rapidly phosphorylated, desensitized and internalized upon ligand activation.

Taken together, we have demonstrated that TUG-891 is a potent and selective agonist for hFFA4 and that this compound does produce many of the therapeutically beneficial effects that have been attributed in the literature to FFA4 activation, at least to some degree. However, we also note significantly reduced selectivity of TUG-891 at mFFA4, which will make using this compound in pre-clinical *in vivo* proof of principle studies extremely challenging if the aim is to define specific roles of mFFA4. Furthermore, the relatively low efficacy of TUG-891 in several measured outputs raises questions as to whether desensitization of this receptor may be an issue. However, TUG-891 does produce a robust increase in GLP-1 secretion in the model systems employed and this indicates that if potential issues with ligand selectivity, response efficacy, and desensitization can be overcome, FFA4 remains an exciting possible target for the treatment of type 2 diabetes and obesity.

MOL # 87783

Authorship contributions

Participated in research design: Hudson, Tobin, and Milligan

Conducted experiments: Hudson, Mackenzie, Butcher, Padiani, and Heathcote

Contributed new reagents or analytic tools: Shimpukade, Christiansen and Ulven

Performed data analysis: Hudson, Butcher, and Padiani

Wrote or contributed to the writing of the manuscript: Hudson and Milligan

MOL # 87783

References

Bartoschek S, Klabunde T, Defossa E, Dietrich V, Stengelin S, Griesinger C, Carlomagno T, Focken I, and Wendt KU (2010) Drug design for G-protein-coupled receptors by a ligand-based NMR method.

Angew Chem Int Ed Engl **49**: 1426–1429.

Briscoe CP, Peat AJ, McKeown SC, Corbett DF, Goetz AS, Littleton TR, McCoy DC, Kenakin TP, Andrews JL, Ammala C, et al. (2006) Pharmacological regulation of insulin secretion in MIN6 cells through the fatty acid receptor GPR40: identification of agonist and antagonist small molecules. *Br J Pharmacol* **148**: 619–628.

Burant CF, Viswanathan P, Marcinak J, Cao C, Vakilynejad M, Xie B, and Leifke E (2012) TAK-875 versus placebo or glimepiride in type 2 diabetes mellitus: a phase 2, randomised, double-blind, placebo-controlled trial. *Lancet* **379**: 1403–1411.

Burns RN, and Moniri NH (2010) Agonism with the omega-3 fatty acids alpha-linolenic acid and docosahexaenoic acid mediates phosphorylation of both the short and long isoforms of the human GPR120 receptor. *Biochem Biophys Res Commun* **396**: 1030–1035.

Christiansen E, Due-Hansen ME, Urban C, Grundmann M, Schröder R, Hudson BD, Milligan G, Cawthorne MA, Kostenis E, Kassack MU, et al. (2012) Free fatty acid receptor 1 (FFA1/GPR40) agonists: mesylpropoxy appendage lowers lipophilicity and improves ADME properties. *J Med Chem* **55**: 6624–6628.

Edfalk S, Steneberg P, and Edlund H (2008) Gpr40 is expressed in enteroendocrine cells and mediates free fatty acid stimulation of incretin secretion. *Diabetes* **57**: 2280–2287.

MOL # 87783

Fukunaga S, Setoguchi S, Hirasawa A, and Tsujimoto G (2006) Monitoring ligand-mediated internalization of G protein-coupled receptor as a novel pharmacological approach. *Life Sci* **80**: 17-23.

Gotoh C, Hong YH, Iga T, Hishikawa D, Suzuki Y, Song SH, Choi KC, Adachi T, Hirasawa A, Tsujimoto G, Sasaki S, and Roh SG (2007) The regulation of adipogenesis through GPR120. *Biochem Biophys Res Commun* **354**: 591-597.

Gregory KJ, Hall NE, Tobin AB, Sexton PM, and Christopoulos A (2010) Identification of orthosteric and allosteric site mutations in M2 muscarinic acetylcholine receptors that contribute to ligand-selective signaling bias. *J Biol Chem* **285**: 7459–7474.

Gregory KJ, Sexton PM, Tobin AB, and Christopoulos A (2012) Stimulus bias provides evidence for conformational constraints in the structure of a G protein-coupled receptor. *J Biol Chem* **287**: 37066–37077.

Groeger AL, Cipollina C, Cole MP, Woodcock SR, Bonacci G, Rudolph TK, Rudolph V, Freeman BA, and Schopfer FJ (2010) Cyclooxygenase-2 generates anti-inflammatory mediators from omega-3 fatty acids. *Nat Chem Biol* **6**: 433–441.

Hara T, Hirasawa A, Sun Q, Sadakane K, Itsubo C, Iga T, Adachi T, Koshimizu T-A, Hashimoto T, Asakawa Y, et al. (2009a) Novel selective ligands for free fatty acid receptors GPR120 and GPR40. *Naunyn Schmiedebergs Arch Pharmacol* **380**: 247–255.

Hara T, Hirasawa A, Sun Q, Koshimizu T-A, Itsubo C, Sadakane K, Awaji T, and Tsujimoto G (2009b) Flow cytometry-based binding assay for GPR40 (FFAR1; free fatty acid receptor 1). *Mol Pharmacol* **75**:

MOL # 87783

85–91.

Hirasawa A, Tsumaya K, Awaji T, Katsuma S, Adachi T, Yamada M, Sugimoto Y, Miyazaki S, and Tsujimoto G (2005) Free fatty acids regulate gut incretin glucagon-like peptide-1 secretion through GPR120. *Nat Med* **11**: 90–94.

Holliday ND, Watson S-J, and Brown AJH (2011) Drug discovery opportunities and challenges at G protein coupled receptors for long chain free Fatty acids. *Front Endocrinol (Lausanne)* **2**: 112.

Hudson BD, Christiansen E, Tikhonova IG, Grundmann M, Kostenis E, Adams DR, Ulven T, and Milligan G (2012a) Chemically engineering ligand selectivity at the free fatty acid receptor 2 based on pharmacological variation between species orthologs. *FASEB J* **26**: 4951–4965.

Hudson BD, Due-Hansen ME, Christiansen E, Hansen AM, Mackenzie AE, Murdoch H, Pandey SK, Ward RJ, Marquez R, Tikhonova IG, Ulven T, Milligan G (2013a) Defining the molecular basis for the first potent and selective orthosteric agonists of the FFA2 free fatty acid receptor. *J Biol Chem* **288**: 17296-17312

Hudson BD, Smith NJ, and Milligan G (2011) Experimental challenges to targeting poorly characterized GPCRs: uncovering the therapeutic potential for free fatty acid receptors. *Adv Pharmacol* **62**: 175–218.

Hudson BD, Tikhonova IG, Pandey SK, Ulven T, and Milligan G (2012b) Extracellular ionic locks determine variation in constitutive activity and ligand potency between species orthologs of the free fatty acid receptors FFA2 and FFA3. *J Biol Chem* **287**: 41195–41209.

Hudson BD, Ulven T, and Milligan G (2013b) The Therapeutic Potential of Allosteric Ligands for Free

MOL # 87783

Fatty Acid Sensitive GPCRs. *Curr Top Med Chem* **13**: 14–25.

Ichimura A, Hirasawa A, Poulain-Godefroy O, Bonnefond A, Hara T, Yengo L, Kimura I, Leloire A, Liu N, Iida K, Choquet H, Besnard P, Lecoecur C, Vivequin S, Ayukawa K, Takeuchi M, Ozawa K, Tauber M, Maffei C, Morandi A, Buzzetti R, Elliott P, Pouta A, Jarvelin MR, Körner A, Kiess W, Pigeyre M, Caiazzo R, Van Hul W, Van Gaal L, Horber F, Balkau B, Lévy-Marchal C, Rouskas K, Kouvatsi A, Hebebrand J, Hinney A, Scherag A, Pattou F, Meyre D, Koshimizu TA, Wolowczuk I, Tsujimoto G, Froguel P. (2012) Dysfunction of lipid sensor GPR120 leads to obesity in both mouse and human. *Nature* **483**: 350–354.

Itoh Y, Kawamata Y, Harada M, Kobayashi M, Fujii R, Fukusumi S, Ogi K, Hosoya M, Tanaka Y, Uejima H, Tanaka H, Maruyama M, Satoh R, Okubo S, Kizawa H, Komatsu H, Matsumura F, Noguchi Y, Shinohara T, Hinuma S, Fujisawa Y, Funjino M (2003) Free fatty acids regulate insulin secretion from pancreatic beta cells through GPR40. *Nature* **422**: 173–176.

Kaku K, Araki T, and Yoshinaka R (2013) Randomized, double-blind, dose-ranging study of TAK-875, a novel GPR40 agonist, in Japanese patients with inadequately controlled type 2 diabetes. *Diabetes Care* **36**: 245–250.

Li H, Ruan XZ, Powis SH, Fernando R, Mon WY, Wheeler DC, Moorhead JF, and Varghese Z (2005) EPA and DHA reduce LPS-induced inflammation responses in HK-2 cells: evidence for a PPAR-gamma-dependent mechanism. *Kidney Int* **67**: 867–874.

Luo J, Swaminath G, Brown SP, Zhang J, Guo Q, Chen M, Nguyen K, Tran T, Miao L, Dransfield PJ, Vimolratana M, Houze JB, Wong S, Toteva M, Shan B, Li F, Zhuang R, Lin DC (2012) A potent class of GPR40 full agonists engages the enteroinsular axis to promote glucose control in rodents. *PLoS ONE* **7**:

MOL # 87783

e46300.

Mobraten K, Haug TM, Kleiveland CR, and Lea T (2013) Omega-3 and omega-6 PUFAs induce the same GPR120-mediated signalling events, but with different kinetics and intensity in Caco-2 cells. *Lipids Health Dis* **12**: 101.

Negoro N, Sasaki S, Mikami S, Ito M, Tsujihata Y, Ito R, Suzuki M, Takeuchi K, Suzuki N, Miyazaki J, Santou T, Odani T, Kanzaki N, Funami M, Morohashi A, Nonaka M, Matsunaga S, Yasuma T, Momose Y (2012) Optimization of (2,3-dihydro-1-benzofuran-3-yl)acetic acids: discovery of a non-free fatty acid-like, highly bioavailable G protein-coupled receptor 40/free fatty acid receptor 1 agonist as a glucose-dependent insulinotropic agent. *J Med Chem* **55**: 3960–3974.

Oh DY, Talukdar S, Bae EJ, Imamura T, Morinaga H, Fan W, Li P, Lu WJ, Watkins SM, and Olefsky JM (2010) GPR120 is an omega-3 fatty acid receptor mediating potent anti-inflammatory and insulin-sensitizing effects. *Cell* **142**: 687–698.

Shenoy SK, Drake MT, Nelson CD, Houtz DA, Xiao K, Madabushi S, Reiter E, Premont RT, Lichtarge O, and Lefkowitz RJ (2006) β -arrestin-dependent, G protein-independent ERK1/2 activation by the beta2 adrenergic receptor. *J Biol Chem* **281**: 1261–1273.

Shimpukade B, Hudson BD, Hovgaard CK, Milligan G, and Ulven T (2012) Discovery of a potent and selective GPR120 agonist. *J Med Chem* **55**: 4511–4515.

Smith NJ, Stoddart LA, Devine NM, Jenkins L, and Milligan G (2009) The action and mode of binding of thiazolidinedione ligands at free fatty acid receptor 1. *J Biol Chem* **284**: 17527–17539.

MOL # 87783

Stoddart LA, Smith NJ, and Milligan G (2008a) International Union of Pharmacology. LXXI. Free fatty acid receptors FFA1, -2, and -3: pharmacology and pathophysiological functions. *Pharmacol Rev* **60**: 405–417.

Stoddart LA, Smith NJ, Jenkins L, Brown AJ, and Milligan G (2008b) Conserved polar residues in transmembrane domains V, VI, and VII of free fatty acid receptor 2 and free fatty acid receptor 3 are required for the binding and function of short chain fatty acids. *J Biol Chem* **283**: 32913–32924.

Sun Q, Hirasawa A, Hara T, Kimura I, Adachi T, Awaji T, Ishiguro M, Suzuki T, Miyata N, Tsujimoto G (2010) Structure-activity relationships of GPR120 agonists based on a docking simulation. *Mol Pharmacol* **78**: 804-810

Suzuki T, Igari S-I, Hirasawa A, Hata M, Ishiguro M, Fujieda H, Itoh Y, Hirano T, Nakagawa H, Ogura M, Makishima M, Tsujimoto G, Miyata N (2008) Identification of G protein-coupled receptor 120-selective agonists derived from PPARgamma agonists. *J Med Chem* **51**: 7640–7644.

Taneera J, Lang S, Sharma A, Fadista J, Zhou Y, Ahlqvist E, Jonsson A, Lyssenko V, Vikman P, Hansson O, Parikh H, Korsgren O, Soni A, Krus U, Zhang E, Jing XJ, Esguerra JL, Wollheim CB, Salehi A, Rosengren A, Renström E, Groop L (2012) A systems genetics approach identifies genes and pathways for type 2 diabetes in human islets. *Cell Metab* **16**: 122–134.

Takasaki J, Saito T, Taniguchi M, Kawasaki T, Moritani Y, Hayashi K, Kobori M (2004) A novel G α_{q11} -selective inhibitor. *J Biol Chem* **279**: 47438-47335.

Tikhonova IG, Sum CS, Neumann S, Thomas CJ, Raaka BM, Costanzi S, and Gershengorn MC (2007) Bidirectional, iterative approach to the structural delineation of the functional “chemoprint” in GPR40 for

MOL # 87783

agonist recognition. *J Med Chem* **50**: 2981–2989.

Ulven T (2012) Short-chain free fatty acid receptors FFA2/GPR43 and FFA3/GPR41 as new potential therapeutic targets. *Front Endocrinol (Lausanne)* **3**: 111.

Wang J, Wu X, Simonavicius N, Tian H, and Ling L (2006) Medium-chain fatty acids as ligands for orphan G protein-coupled receptor GPR84. *J Biol Chem* **281**: 34457–34464.

Watson S-J, Brown AJH, and Holliday ND (2012) Differential signaling by splice variants of the human free fatty acid receptor GPR120. *Mol Pharmacol* **81**: 631–642.

MOL # 87783

Footnotes

These studies were funded in part by grants from the Biotechnology and Biosciences Research Council [BB/K019864/1] (to GM), and [BB/K019856/1] (to ABT), core funding from the MRC Toxicology Unit (to ABT), the Danish Council for Strategic Research 11-116196 (to TU and GM) and the Canadian Institutes of Health Research (fellowship to BDH).

MOL # 87783

Legends for Figures

Figure 1. *TUG-891 is a potent agonist of FFA4.* Chemical structures of the ligands: aLA, GW9508, NCG21 and TUG-891 are in **A**. Concentration-response data for each agonist at hFFA4 are shown in Ca^{2+} mobilization (**B**), β -arrestin-2 recruitment (**C**) and ERK phosphorylation (**D**) assays. ‘Bias plots’ are also shown comparing responses to equal concentrations of each ligand between β -arrestin-2 recruitment and ERK phosphorylation (**E**), β -arrestin-2 recruitment and Ca^{2+} mobilization (**F**), or ERK phosphorylation and Ca^{2+} mobilization (**G**) assays. On these plots, a theoretical relationship for a complete lack of bias between pathways is shown in the dashed line.

Figure 2. *FFA4 activates ERK phosphorylation primarily through $G_{q/11}$ mediated pathways.* Time course pERK analysis was carried out in hFFA4-eYFP Flp-InTM T-RExTM 293 cells in response to aLA (300 μM ; black circles), TUG-891 (10 μM ; dark grey squares), or FBS (10%; light grey triangles) are shown in **A**. In **B**. 5 min pERK responses to aLA (300 μM ; black), TUG-891 (10 μM ; dark grey), and FBS (10%; light grey) are shown from control, YM-254890 (YM, 100 nM), or Iressa (1 μM) pretreated cells. * $p < 0.05$, *** $p < 0.001$ compared with control for the same ligand. Similar experiments are shown in **C**. following 15 min treatment with either aLA (300 μM ; black) or TUG-891 (10 μM ; dark grey). In this graph the dashed line indicates the basal pERK level. ** $p < 0.01$, *** $p < 0.001$ compared with control for the same ligand. In **D**. the effect of Iressa (10 μM) pre-treatment on the EGF receptor pERK response is shown; *** $p < 0.001$. **E** shows the Ca^{2+} response to TUG-891 without or with YM (100 nM) pretreatment. In **F**. pERK responses after 5 min treatment with aLA (300 μM , black), TUG-891 (10 μM , dark grey), or FBS (10%; light grey) are shown in either untransfected cells (untreated); cells transfected with control non-targeting siRNA (control); or cells transfected with β -arrestin-2 targeting siRNA (β -Arr-2). Inset shows RT-PCR results using β -arrestin-2 primers for reactions either with no template (NTC), or using RNA isolated from control or β -arrestin-2 siRNA transfected cells, each carried out either without or with reverse transcriptase (RT) enzyme. Fluorescent microscopy of either control or β -arrestin-2 siRNA

MOL # 87783

transfected cells treated with vehicle or TUG-891 (10 μ M; 45 min) is in **G**. Scale bar is 100 μ m. High content imaging results for TUG-891 (10 μ M; 45 min) mediated internalization in control or β -arrestin-2 siRNA transfected cells are shown in **H**; *** $p < 0.001$.

Figure 3. *FFA4 is rapidly internalized, phosphorylated and desensitized following treatment with TUG-891.* Internalization of an eYFP tagged form of hFFA4 was monitored by spinning disk confocal microscopy in live cells at 5 min intervals following treatment with either aLA (100 μ M) (**A**) or TUG-891 (10 μ M) (**B**). Quantitative assessment of the kinetics of internalization using a high-content imaging assay is shown in **C**. In **D** concentration-response curves were generated using each FFA4 agonist in the high-content internalization assay after a 45 min ligand incubation. Phosphorylation of an hFFA4 construct containing an HA tag at the C terminus was assessed by [32 P] incorporation, followed by immunoprecipitation for the HA tag (**E**). A representative [32 P] autoradiograph (upper panel) and anti-HA immunoblot (lower panel) are shown and polypeptides corresponding to the predicted size of hFFA4-HA are marked. Quantification of the [32 P] autoradiograph is in **F**. Tryptic phosphopeptide maps are shown in **G**. A representative trace from single cell Ca^{2+} imaging desensitization experiments is shown in **H**.

Figure 4. *FFA4 is rapidly recycled back to the cell surface and resensitized after removal of TUG-891.* Fluorescence microscopy images of hFFA4-eYFP Flp-InTM T-RExTM 293 cells treated for 45 min with DMSO vehicle (0.1%) or TUG-891 (10 μ M), washed, then either fixed immediately (0 min recovery) or allowed to recover for 60 min before fixing and imaging are shown in **A**. Scale bar represents 100 μ m. Time course experiments were conducted in these cells measuring total FFA4-eYFP expression (**B**), cell surface FFA4-eYFP expression (**C**) (***) $p < 0.001$ compared with vehicle treatment), and internalized FFA4-eYFP (**D**), in 10 min intervals after first treating with DMSO vehicle (0.1%) or TUG-891 (10 μ M) for 45 min. In **E**, parallel experiments where cells were treated with either DMSO vehicle (0.1%, black bars), or TUG-891 (10 μ M, grey bars) for 45 min, before washing and then measuring the acute Ca^{2+}

MOL # 87783

response to TUG-891 (10 μ M) at 10 min intervals. *** $p < 0.001$, * $p < 0.05$ compared with acute TUG-891 response measured in vehicle desensitized cells at the same time point. Correlations are shown between internalized receptor and cell surface expression (**F**), cell surface expression and Ca^{2+} response (**G**), and internalized receptor and Ca^{2+} response (**H**). In **G** and **H** fit lines were segmented at 50% cell surface expression, and 40% internalized receptor respectively.

Figure 5. *TUG-891 is an orthosteric agonist of FFA4.* Concentration-response curves are shown for aLA (**A**) and TUG-891 (**B**) at wild-type, R99Q and R178Q mutants of hFFA4 measured using the β -arrestin-2 recruitment assay in transiently transfected HEK293T cells. In **C** quantitative measures of cell surface and total receptor expression for each mutant are shown.

Figure 6. *TUG-891 is selective for hFFA4 over hFFA1.* Concentration-response curves for aLA (**A**), GW9508 (**B**), NCG21 (**C**) and TUG-891 (**D**) in β -arrestin-2 recruitment BRET assays conducted in transiently transfected HEK293T cells are shown for hFFA4 (black lines) and hFFA1 (grey lines). Concentration-response data are also shown for NCG21 (**E**) and TUG-891 (**F**) in Flp-InTM T-RExTM cells induced to express hFFA4 (black lines) or hFFA1 (grey lines) in Ca^{2+} mobilization assays.

Figure 7. *TUG-891 produces signaling responses in HT-29 cells.* Expression of FFA4 and FFA1 mRNA was assessed by RT-PCR in the HT-29 human adenocarcinoma cell line (**A**). Concentration-response data in HT-29 cells are shown for Ca^{2+} and ERK phosphorylation assays in **B** and **C** respectively.

Figure 8. *TUG-891 is a potent agonist of mFFA4, but shows only limited assay-dependent selectivity over mFFA1.* In **A**, concentration-response data are shown for various FFA4 agonists in the β -arrestin-2 recruitment assay utilizing HEK293T cells transiently transfected with mFFA4. **B** and **C** show concentration-response data for TUG-891 at mFFA4 (black lines) and mFFA1 (grey lines) in β -arrestin-2

MOL # 87783

recruitment (transiently transfected HEK293T cells) and Ca^{2+} mobilization (Flp-InTM T-RExTM 293 stable inducible cells) assays respectively. Concentration-response data for the FFA1 selective agonist, TUG-905, are shown in **D** for both mFFA4 (black lines) and mFFA1 (grey lines). Inhibition experiments are shown in **E** utilizing Flp-InTM T-RExTM 293 cells expressing mFFA1 and fixed concentrations of TUG-905 (100 nM), TUG-891 (3 μM) or aLA (3 μM) with increasing concentrations of the FFA1 antagonist GW1100.

Figure 9. TUG-891 and aLA stimulate GLP-1 release primarily through activation of FFA4. The expression of FFA1 and FFA4 mRNA was assessed in both STC-1 and GLUTag enteroendocrine cell lines (**A**). The secretion of GLP-1 was assessed in STC-1 (**B**) and GLUTag (**C**) cells treated with either vehicle (open bars); ligand: aLA (100 μM), TUG-891 (30 μM), or TUG-905 (10 μM) (black bars); or ligand and GW1100 (10 μM). *** $p < 0.001$, ** $p < 0.01$ compared with vehicle treatment. ** $p < 0.01$ compared with ligand without GW1100 treatment.

Figure 10. TUG-891 stimulates glucose uptake in 3T3-L1 adipocytes and inhibits TNF secretion from RAW 264.7 macrophages. In **A**, [³H]deoxyglucose uptake was measured in differentiated 3T3-L1 adipocytes in response to single concentrations of aLA (100 μM), TUG-891 (10 μM) and insulin (1 μM). *** $p < 0.001$, * $p < 0.05$. Concentration-response data were generated for aLA (**B**) and TUG-891 (**C**), with calculated EC_{50} values shown. The ability of aLA (100 μM), TUG-891 (10 μM), TUG-905 (10 μM) and DHA (100 μM) to inhibit LPS-stimulated TNF secretion from RAW 264.7 macrophages is shown in **D**. Concentration-response data and the determined potency of aLA and TUG-891 to inhibit TNF secretion are shown in **E** and **F** respectively.

MOL # 87783

Tables

Table 1. pEC₅₀ potency values of agonists at hFFA4 in various functional assays

Assay	aLA	GW9508	NCG21	TUG-891
Ca ²⁺	5.25 ± 0.10	6.07 ± 0.08	5.21 ± 0.11	6.93 ± 0.07
β-arrestin-2	5.29 ± 0.05	6.04 ± 0.04	5.64 ± 0.03	7.19 ± 0.07
β-arrestin-1	4.86 ± 0.05	5.64 ± 0.04	ND	6.83 ± 0.06
pERK	4.08 ± 0.14	5.06 ± 0.25	<4.5	5.83 ± 0.12
Internalization	4.76 ± 0.11	5.25 ± 0.10	5.51 ± 0.18	7.29 ± 0.12

ND- not determined

Figure 1

Molecular Pharmacology Fast Forward. Published on August 26, 2013 as DOI: 10.1124/mol.113.087783
This article has not been copyedited and formatted. The final version may differ from this version.

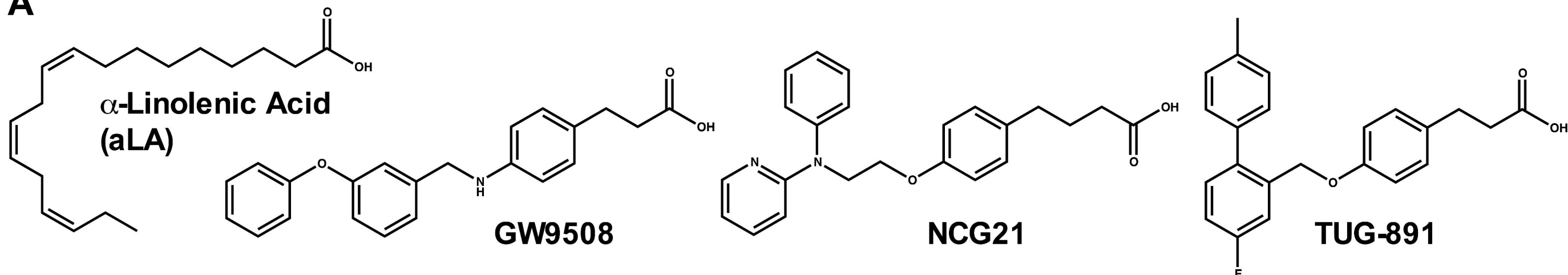
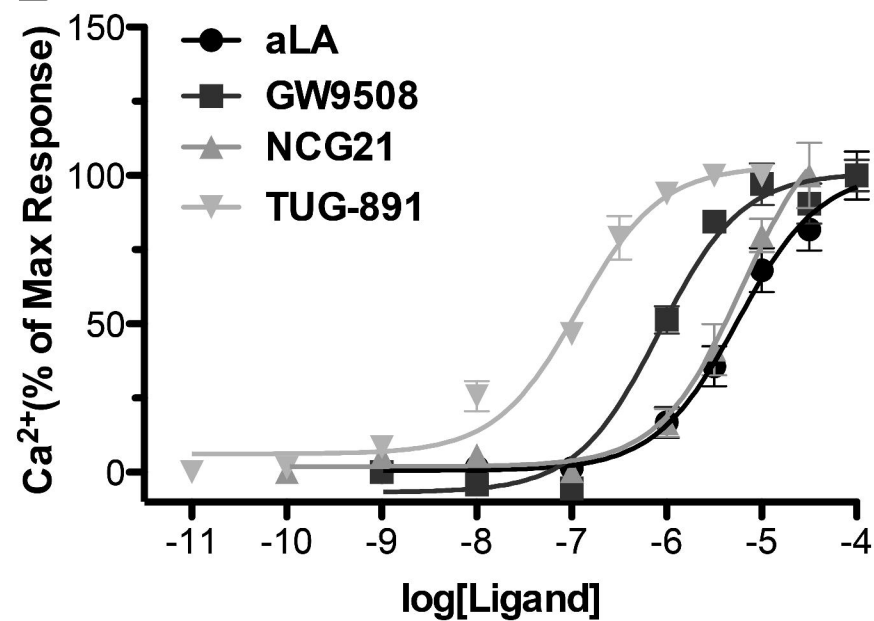
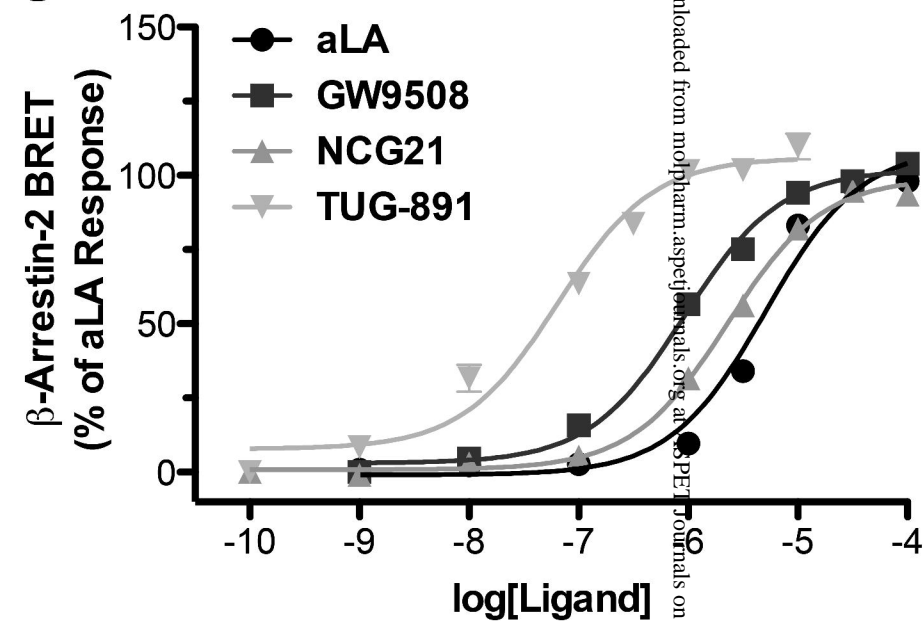
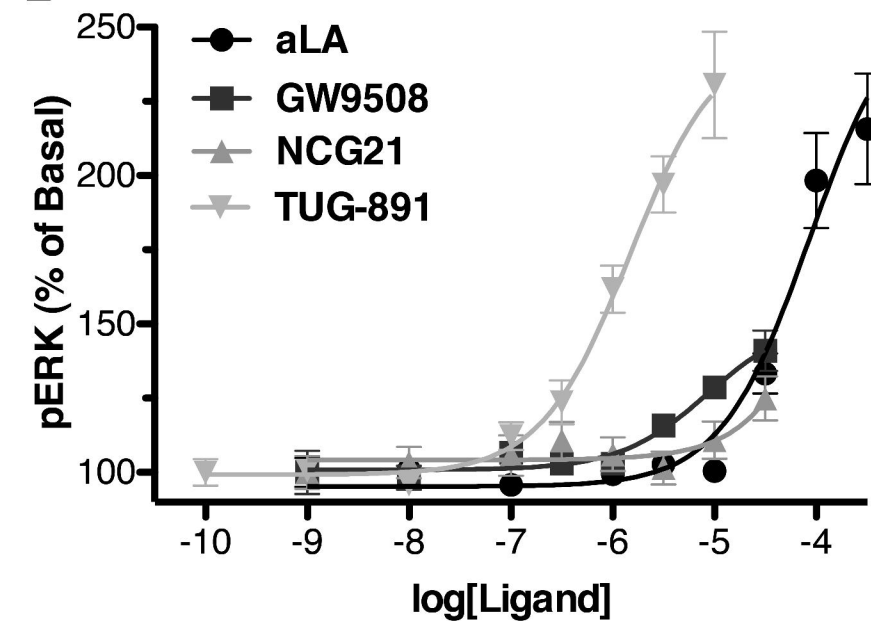
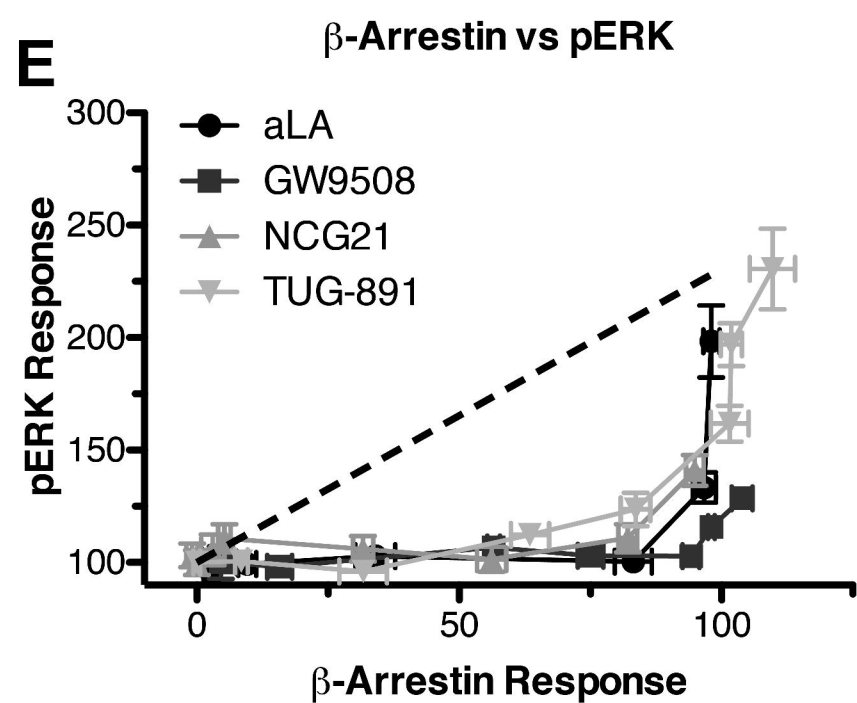
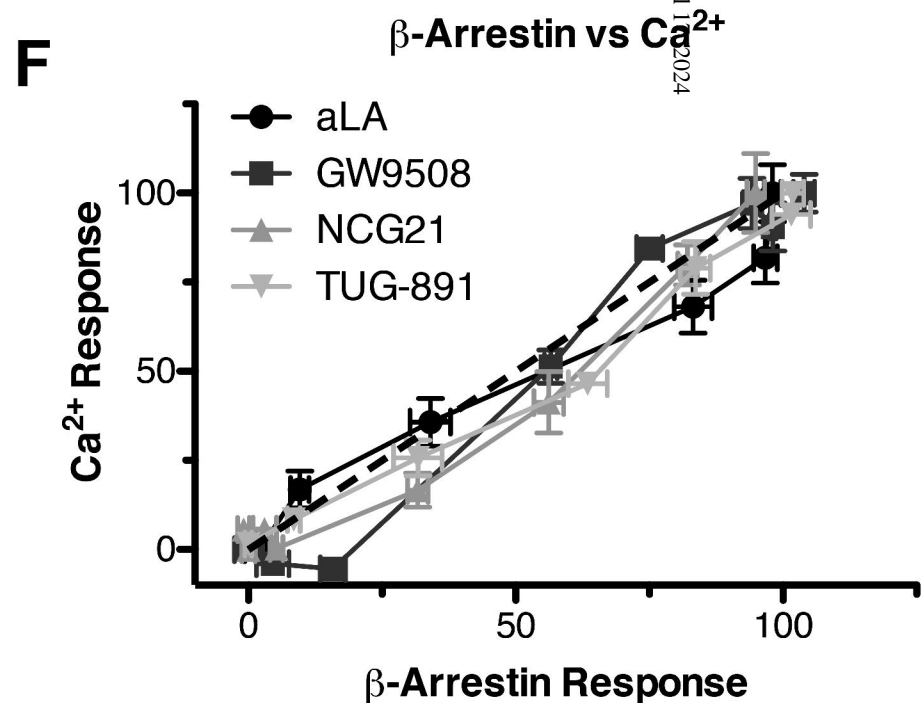
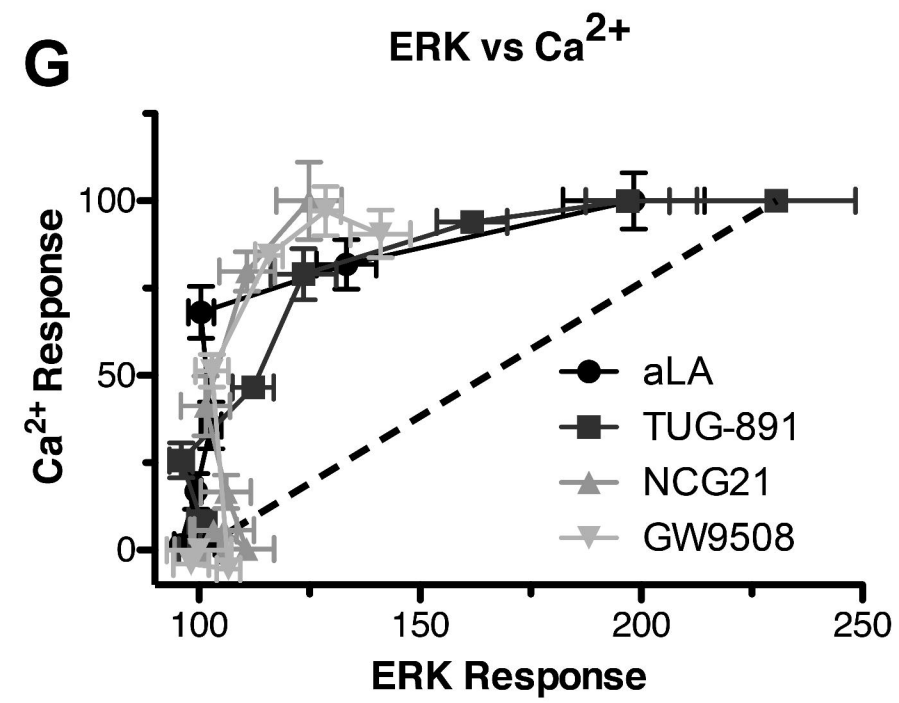
A**B****C****D****E****F****G**

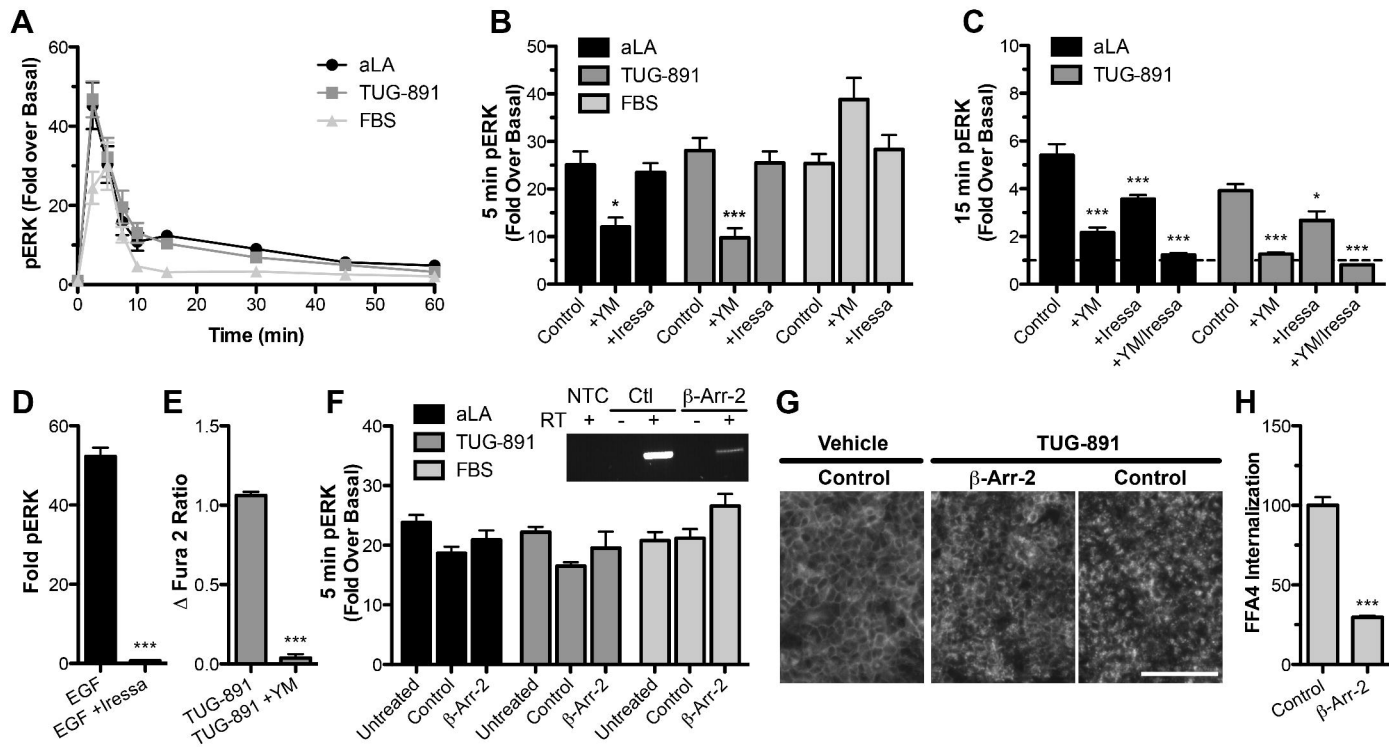
Figure 2

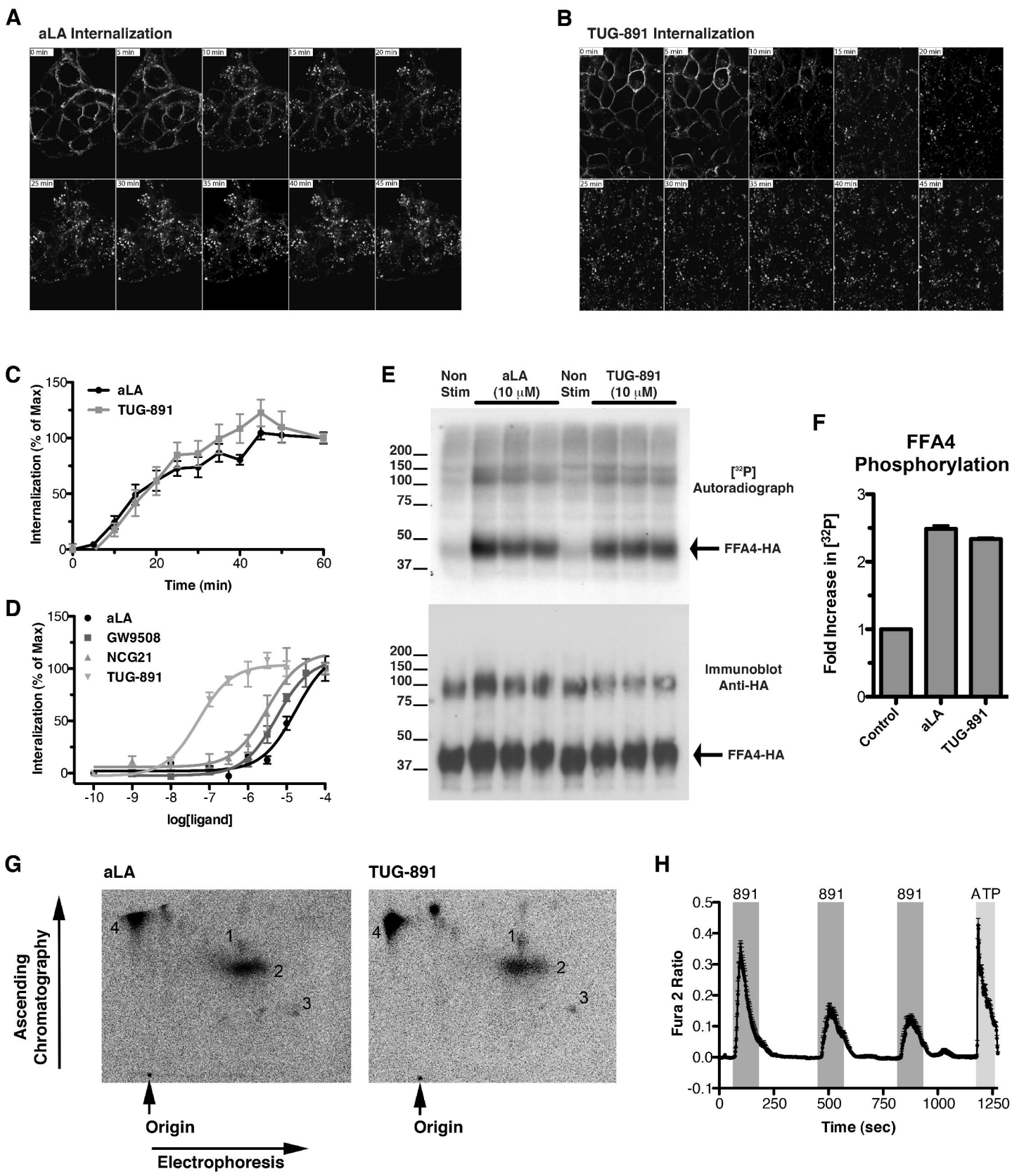
Figure 3

Figure 4

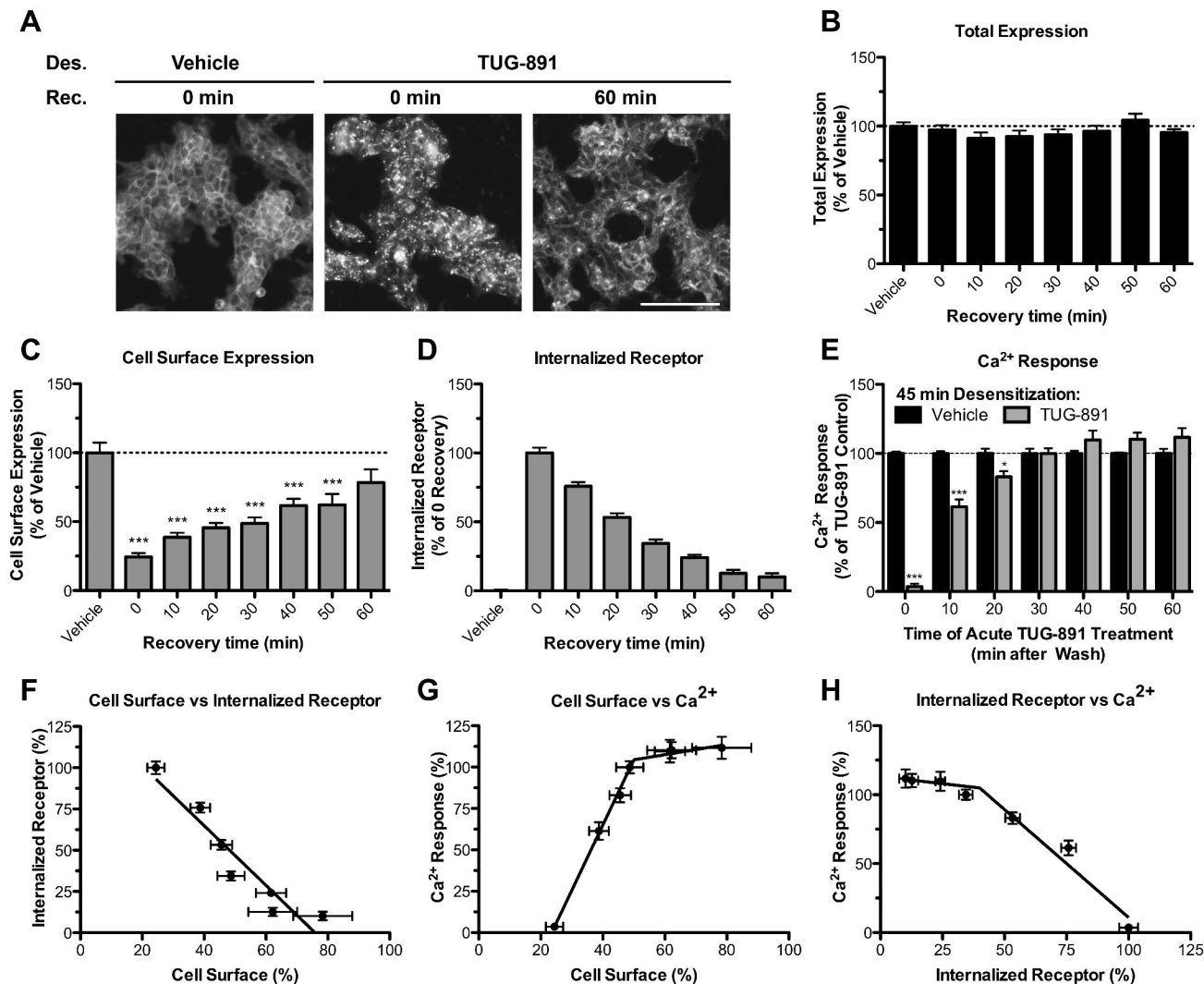


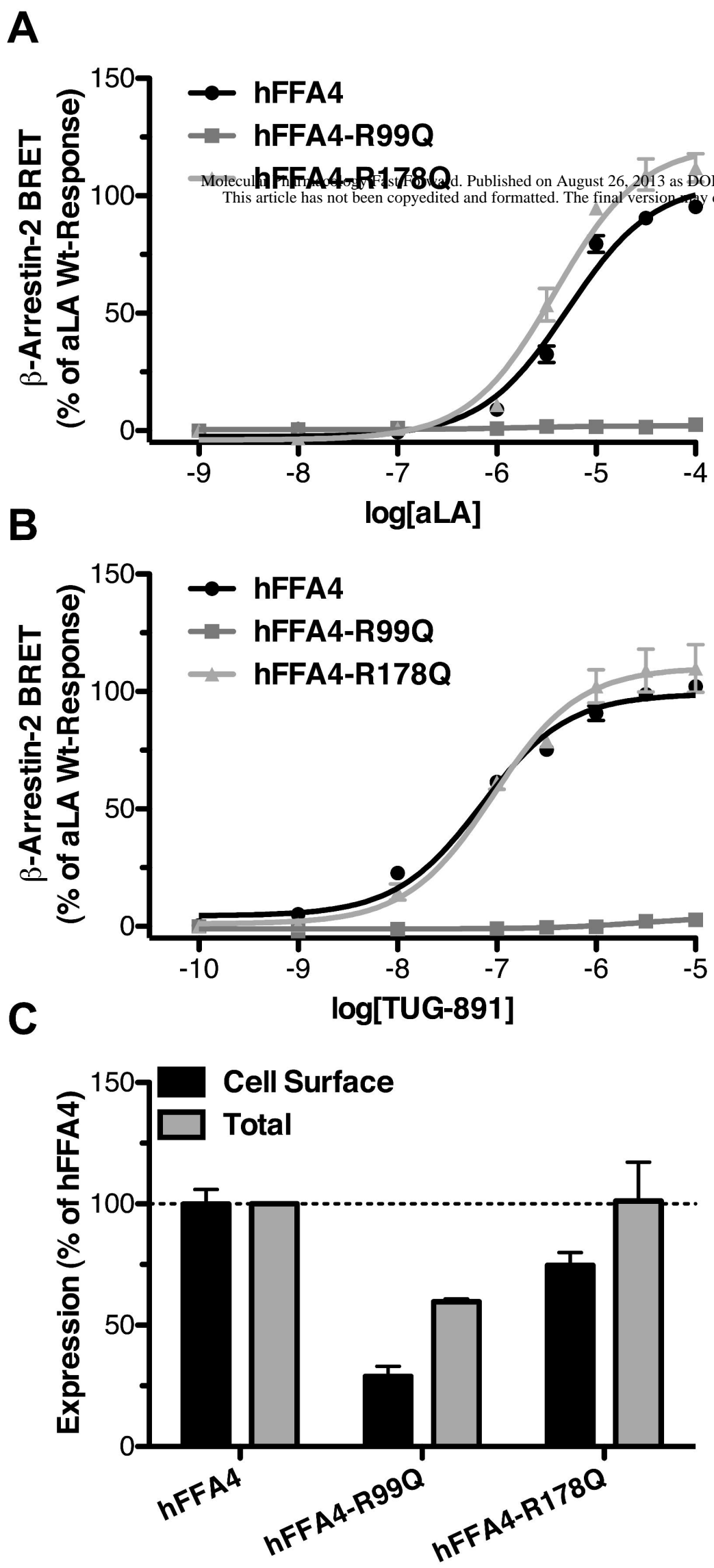
Figure 5

Figure 6

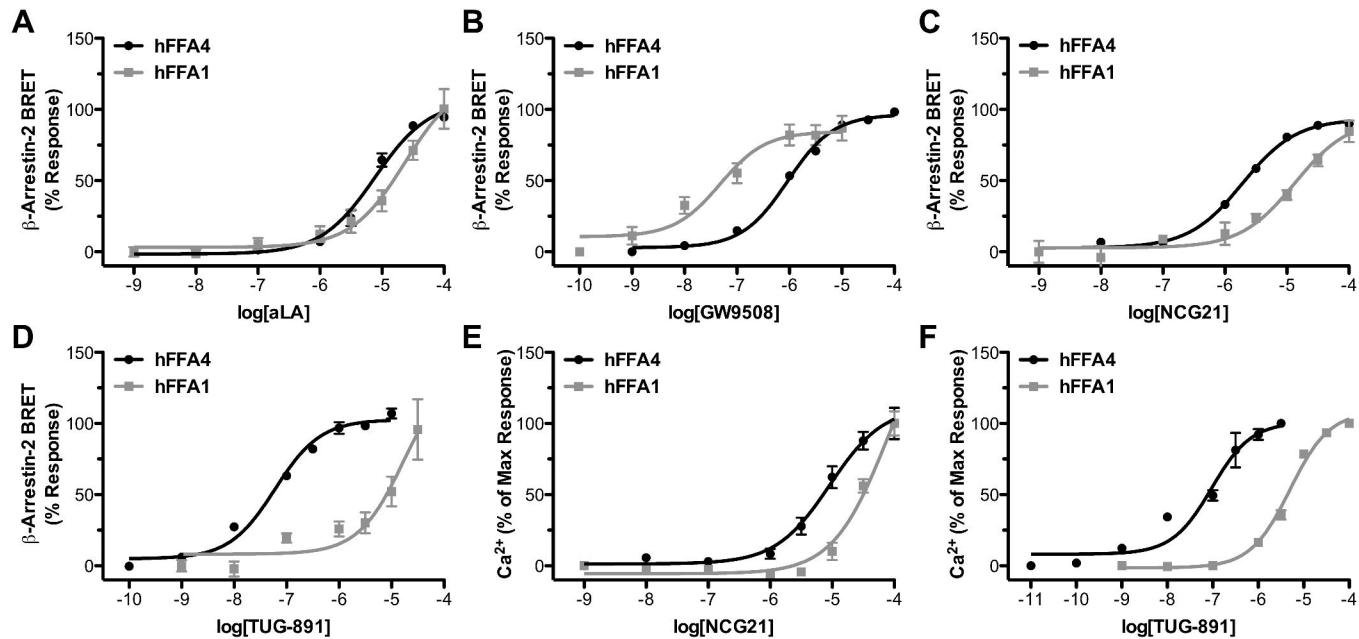
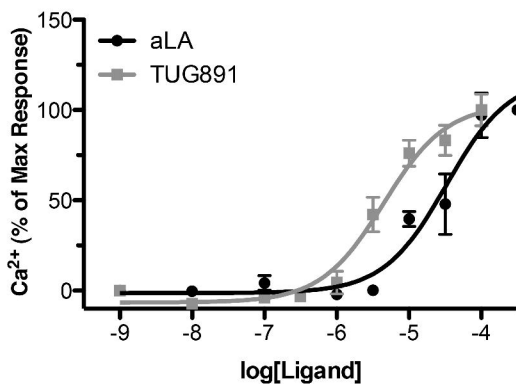


Figure 7

A



B



C

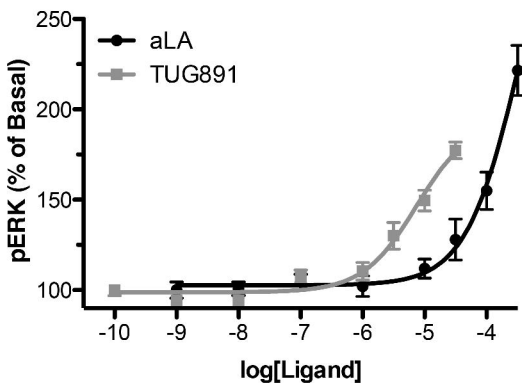
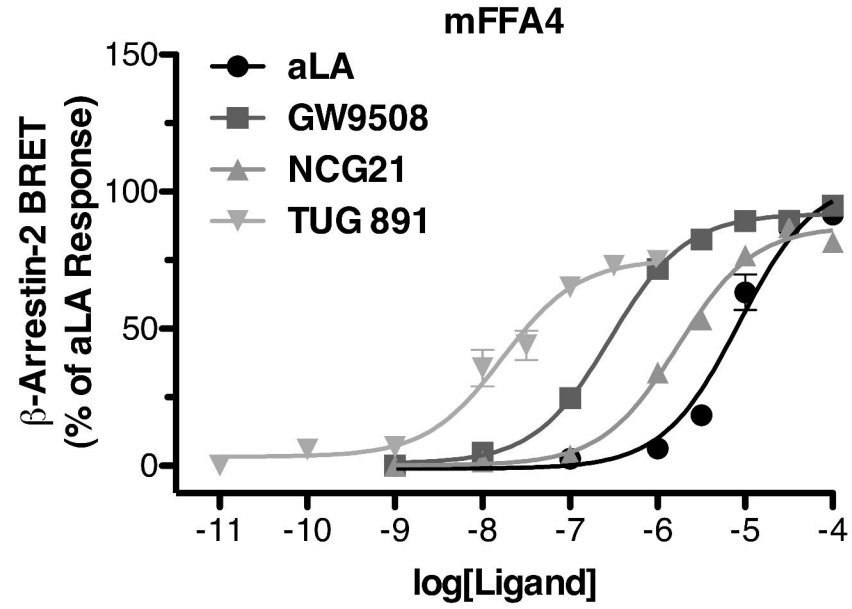
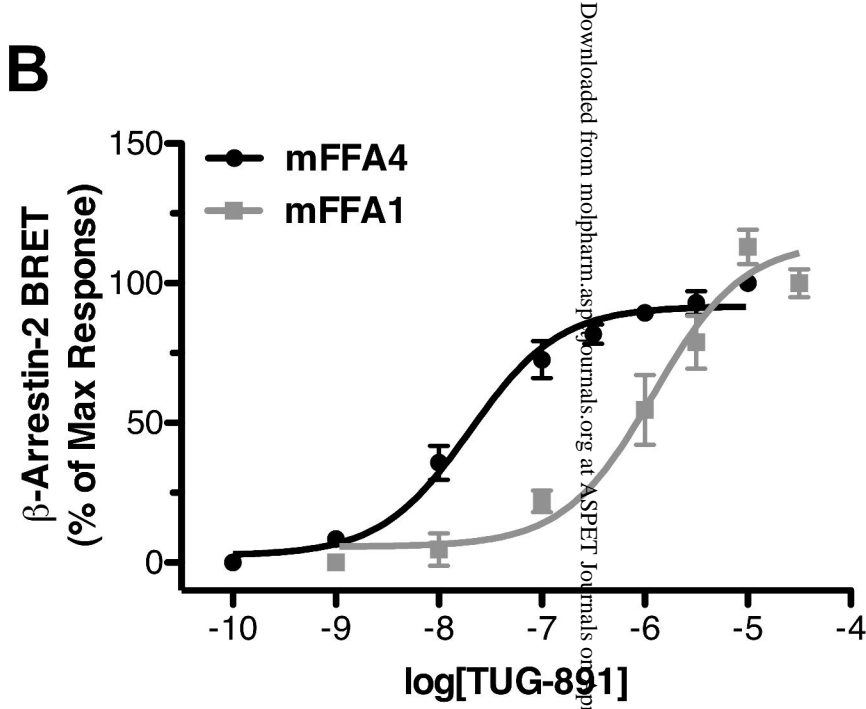


Figure 8

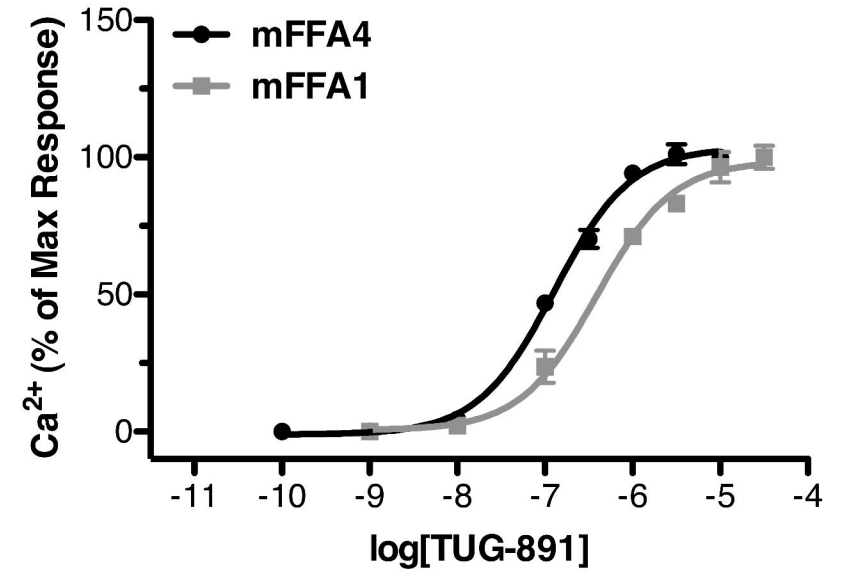
A



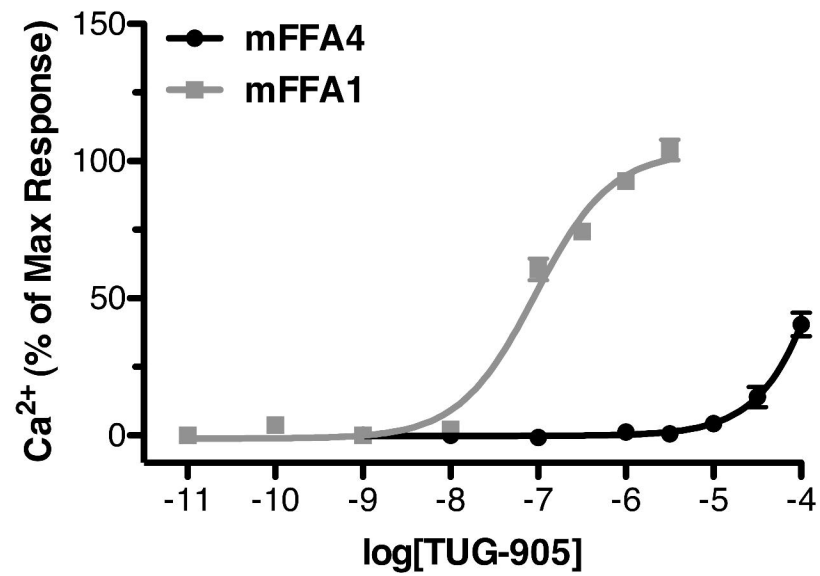
B



C



D



E

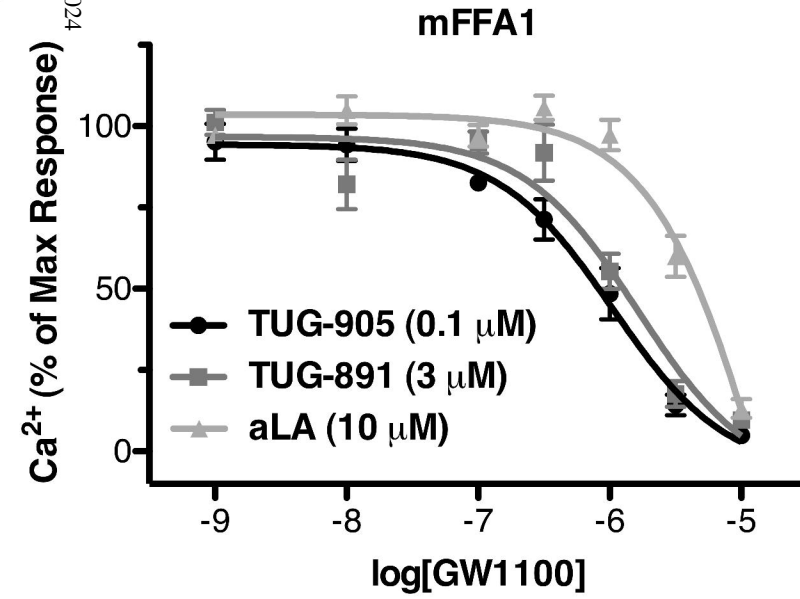


Figure 9

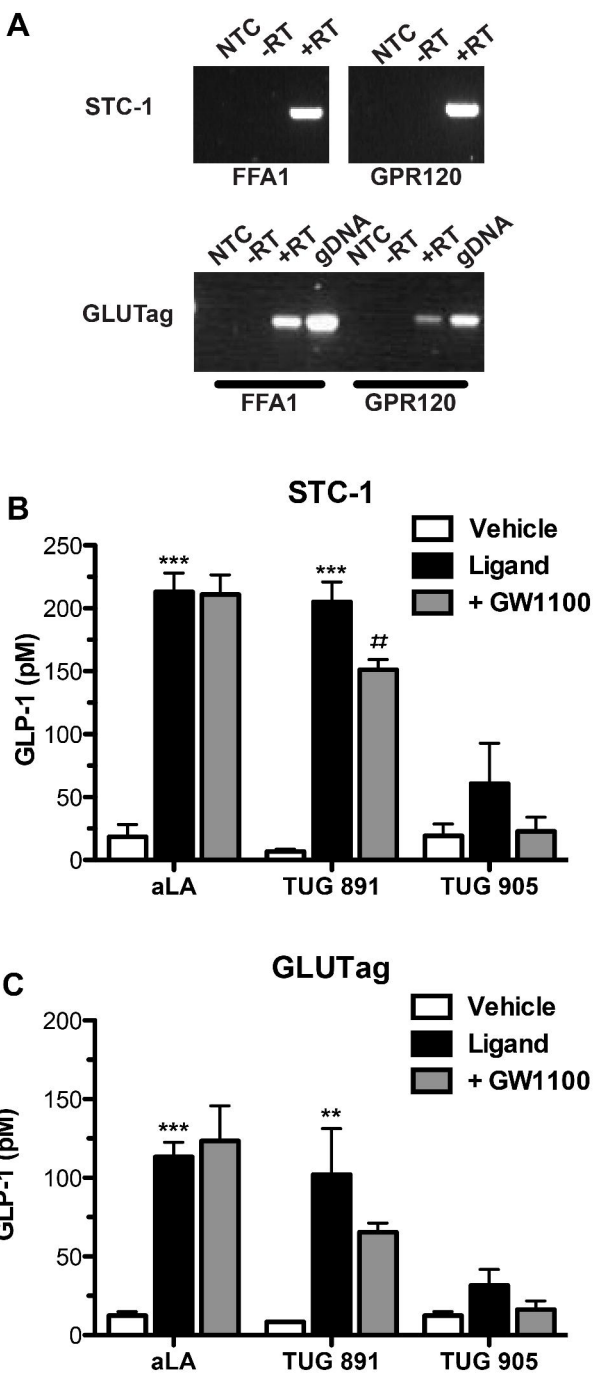


Figure 10

